



OPEN

## Identifying a novel Mecp2-mediated epigenetic mechanism controlling Lonp1 in the hippocampus and its disruption by aging

Jesús Llanquino-Sandoval<sup>1,2,3,10</sup>, Karina A. Cicali<sup>1,2</sup>, Claudia Jara<sup>1,9</sup>, Carlos Vigil-Vásquez<sup>1,2</sup>, Marcela K. Sjöberg-Herrera<sup>7</sup>, Micaela Ricca<sup>4</sup>, Sebastian Valenzuela<sup>4,5</sup>, Alejandra Loyola<sup>2,4</sup>, Marcello Pinti<sup>6</sup>, Andreas Schüller<sup>7,8</sup>, Bredford Kerr<sup>3</sup>✉ & Cheril Tapia-Rojas<sup>1,2</sup>✉

Aging is characterized by a progressive decline in cellular function, including the hippocampus, a brain region crucial for learning and memory. Mitochondrial dysfunction is a hallmark of aging, critical for hippocampal deterioration. The mitochondrial protease Lonp1 is a key regulator of mitochondrial proteostasis, and its diminished expression or activity has been implicated in age-related dysfunction in non-neuronal cells. However, despite its essential role in maintaining mitochondrial function, the transcriptional regulation of Lonp1 remains poorly understood. Evidence suggests that Lonp1 is subject to epigenetic control via changes in DNA methylation patterns. Mecp2, a DNA-methylation reader, acts as a transcriptional regulator highly expressed in neurons, either activating or repressing gene expression. Yet, its role in the mitochondria of aged hippocampus and its potential role as Lonp1 regulator haven't been explored. Here, we investigated Lonp1 expression and its epigenetic regulation by Mecp2 in the hippocampus of aged SAMP8 mice. We identified CpG islands in the *Lonp1* promoter, near the transcription start site, where DNA methylation levels increase in aged hippocampal tissue. Chromatin immunoprecipitation revealed that Mecp2 directly binds to the *Lonp1* promoter, with a significant reduction in binding observed in aged mice, correlating with increased Lonp1 mRNA levels. These findings show, for the first time, that Mecp2 is a transcriptional repressor of Lonp1 in the hippocampus. Additionally, unlike humans expressing three isoforms of *Lonp1*, mice exhibit only the full-length mitochondrial isoform. Interestingly, despite increased *Lonp1* mRNA levels in aged mice, their protein levels were significantly decreased in the aged hippocampus. This unexpected result is, at least in part, explained by the enhanced Lonp1 protein degradation by the lysosome. Together, our findings reveal a novel mechanism that drives Lonp1 expression, linking Mecp2-mediated epigenetic regulation to age-related mitochondrial dysfunction. This study reveals Mecp2 and Lonp1 as potential therapeutic targets for mitochondrial proteostasis in aging.

**Keywords** Aging, Hippocampus, Epigenetics, Mecp2, Lonp1

<sup>1</sup>Laboratory of Neurobiology of Aging, Centro Científico y Tecnológico de Excelencia Ciencia & Vida, Fundación Ciencia & Vida, Huechuraba, 8580702 Santiago, Chile. <sup>2</sup>Facultad de Ciencias, Universidad San Sebastián, Lota 2465, 7510157 Santiago, Chile. <sup>3</sup>Laboratory of Neuroendocrinology and Metabolism, Centro de Biología Celular y Biomedicina (CEBICEM), Facultad de Ciencias, Universidad San Sebastián, Santiago, Chile. <sup>4</sup>Centro Científico y Tecnológico de Excelencia Ciencia & Vida, Fundación Ciencia & Vida, Avenida del Valle Norte 725, Huechuraba, 8580702 Santiago, Chile. <sup>5</sup>Facultad de Medicina Veterinaria, Universidad San Sebastián, Bellavista 07, Recoleta, 8420524 Santiago, Chile. <sup>6</sup>Department of Life Sciences, University of Modena and Reggio Emilia, 41125 Modena, Italy. <sup>7</sup>School of Biological Sciences, Pontificia Universidad Católica de Chile, 8331150 Santiago, Chile. <sup>8</sup>Institute for Biological and Medical Engineering, Pontificia Universidad Católica de Chile, 7820436 Santiago, Chile. <sup>9</sup>Facultad de Salud y Ciencias Sociales, Universidad de Las Américas, 7500975 Santiago, Chile. <sup>10</sup>Present address: Translational Medicine Laboratory, Instituto Oncológico Fundación Arturo López Pérez, 7500691 Santiago, Chile. ✉email: Bredford.kerr@uss.cl; cheril.tapia@uss.cl

Aging is a biological process marked by the progressive accumulation of cellular, tissue, and organ damage, including that of the brain<sup>1–3</sup>. Among the most vulnerable brain regions is the hippocampus, which undergoes functional decline with age<sup>4,5</sup>, leading to impairments in reasoning, processing speed, and memory<sup>4</sup>. A key contributor to this age-related hippocampal deterioration is oxidative stress and the accumulation of abnormal proteins within mitochondria, both of which promote mitochondrial dysfunction, a recognized hallmark of aging<sup>6,7</sup>. Mitochondria generate ATP through oxidative phosphorylation (OXPHOS), a crucial process for maintaining cognitive functions in the hippocampus<sup>8,9</sup>. However, increased oxidative stress and impaired quality control mechanisms render mitochondria particularly susceptible to dysfunction in the brain during aging<sup>8,10,11</sup>.

Mitochondria contain several proteases responsible for maintaining protein homeostasis, including members of the AAA + (ATPases Associated with diverse cellular Activities) superfamily<sup>12,13</sup>. Among them, the Lonp1 protease plays a particularly crucial role in preserving the integrity of the mitochondrial proteome<sup>14</sup>. Lonp1 is localized in the mitochondrial matrix and is ubiquitously expressed across all cell types and tissues<sup>15</sup>. Remarkably, it is estimated that Lonp1 mediates the degradation of over 50% of mitochondrial proteins<sup>16,17</sup>. To that end, Lonp1 selectively targets a range of substrates, including subunits of complexes I and V of the electron transport chain, thus contributing to the remodeling and stabilization of OXPHOS<sup>18,19</sup>. In addition to its proteolytic function, Lonp1 is also involved in maintaining mitochondrial DNA (mtDNA)<sup>20,21</sup>, regulating the stability of mitochondrial transcription factor A (TFAM), and interacting with mitochondrial polymerase  $\gamma$  to support mtDNA replication and transcription<sup>22,23</sup>. These functions underscore the crucial role of Lonp1 in maintaining both mitochondrial structure and bioenergetic capacity. The critical nature of Lonp1 is further demonstrated by the fact that its complete deletion in embryos is lethal. At the same time, heterozygous mice exhibit significant mitochondrial abnormalities, including altered morphology and impaired bioenergetic function in colon enterocytes and embryonic fibroblasts<sup>15,24</sup>. It is well supported that Lonp1 also plays critical roles during adulthood and in aging. Indeed, expression and activity of mitochondrial Lonp1 decline with age in multiple tissues, contributing to mitochondrial proteostasis failure, oxidative stress, and functional defects<sup>25–28</sup>. In aged kidneys, for example, reduced Lonp1 correlates with organ dysfunction and mitochondrial abnormalities<sup>29</sup>. Moreover, in models of muscle disuse and neurodegeneration, loss or impairment of Lonp1 accelerates features of aging and mitochondrial dysfunction<sup>30</sup>. These observations indicate that Lonp1 plays a crucial role in maintaining mitochondrial function in adult and aging tissues. However, despite its well-established roles in peripheral tissues, the function of Lonp1 in brain cells, particularly within the hippocampus, a region crucial for learning and memory, and in the context of aging, remains unexplored.

Additionally, the expression and regulation of the Lonp1 gene remain poorly understood. In humans, Lonp1 exists in three isoforms, generated through RNA alternative splicing<sup>31,32</sup>. Transcript variant 1 contains the mitochondrial-targeting sequence (MTS) and does not undergo splicing, whereas variants 2 and 3 result from differential splicing of exon 1, leading to potential differences in subcellular localization and function. However, the presence of these Lonp1 isoforms in mouse cells has not yet been confirmed. Additionally, several regulators of Lonp1 expression have been identified. These include transcription factors such as Nuclear Respiratory Factor 2 (NRF-2)<sup>33,34</sup>. Moreover, Sirtuin-1, although not a transcription factor itself, can modulate Lonp1 transcription indirectly through the deacetylation and activation of PGC1 $\alpha$ , which in turn stimulates NRF-2 signaling<sup>35</sup>. Nonetheless, the full spectrum of transcriptional regulators of *Lonp1* in the brain, particularly within the context of aging, remains largely unexplored. This highlights a critical unresolved question in understanding how Lonp1 expression is controlled in neuronal tissues and across different species.

Epigenetic modifications of histones and DNA influence gene expression during aging<sup>36</sup>. In humans, the *LONP1* gene undergoes methylation changes at CpG sites in response to environmental factors, such as nitrogen dioxide pollution<sup>37</sup>. Moreover, hypomethylation of a *LONP1* enhancer region has been reported and linked to pathological conditions such as myalgic encephalomyelitis/chronic fatigue syndrome (ME/CFS)<sup>38</sup>. This evidence suggests that epigenetic regulation of *LONP1* is responsive to genome–environment interactions. Mecp2 is the most abundantly expressed member of the methylated DNA-binding protein family in the brain<sup>36,39</sup>. Mutations in Mecp2 have been shown to alter the expression of genes involved in mitochondrial function<sup>40</sup>. Supporting this, deep RNA sequencing of hippocampal tissue from wild-type and Mecp2 knockdown rats revealed changes in the expression of mitochondrial proteases, including the serine protease Htra2 and the ATP-dependent protease Clpx<sup>41</sup>. These findings suggest that Mecp2 may regulate nuclear genes encoding mitochondrial proteins, such as Lonp1. However, whether Mecp2 modulates Lonp1 expression and whether this regulation is influenced by aging remains unknown, as this has not yet been investigated.

In this study, we investigated the age-related regulation of Lonp1 expression and proteostasis in the hippocampus, with a focus on the transcriptional role of Mecp2. Our findings uncover previously unrecognized epigenetic mechanisms involved in Lonp1 regulation during aging. Specifically, we observed increased cytosine DNA methylation in the Lonp1 promoter region. Notably, we demonstrate for the first time that Mecp2 directly binds to the Lonp1 promoter, and that this interaction is significantly reduced in the aged hippocampus. This reduction contrasts with the observed increase in Lonp1 mRNA levels, suggesting that Mecp2 functions as a transcriptional repressor of Lonp1. Furthermore, we report an age-associated decrease in total Mecp2 protein and its phosphorylated form (pSer80) in the nuclear fraction of the hippocampus, potentially explaining Mecp2 diminished capacity to bind and regulate Lonp1. Additionally, in contrast to human cells, we found that only Lonp1 transcript variant 1, the isoform encoding the full-length mitochondrial-targeted protein, is expressed in the hippocampus and other energy-demanding tissues of SAMP8 mice. Finally, despite increased Lonp1 mRNA levels in aging, we observed a paradoxical decrease in Lonp1 protein levels, which we attribute, at least in part, to lysosome-mediated degradation in aged tissue. Collectively, our results reveal a novel methylation-dependent transcriptional regulation of Lonp1 by Mecp2 and identify a critical disconnect between Lonp1 mRNA and protein expression in aging. These findings provide new insight into the molecular mechanisms linking mitochondrial proteostasis and epigenetic regulation in age-related hippocampal dysfunction.

## Materials and methods

### Animals

SAMP8 mice (Senescence-Accelerated Mouse Prone 8) and SAMR1 (Senescence-Accelerated Mouse Resistant 1) 2- and 7-month-old (mo) females were handled according to National Institutes of Health (NIH, Baltimore, MD) guidelines. This study was reported under ARRIVE guidelines. Animals were housed in temperature-controlled cages (24 °C) on a 12-h light/dark cycle, with food and water available ad libitum. The Bioethics and Biosafety Committee of the Universidad San Sebastián, Chile, approved all experimental procedures described in this study (CEC N° 23–2021-20 and 0001–04–04–22). Animals were anesthetized with isoflurane and euthanized via decapitation. At the time of euthanasia, SAMP8 and SAMR1 mice were 2-month-old (25–28 g) or 7-month-old (30–35 g). The hippocampus was dissected for biochemical analysis. Each group consisted of almost three animals for biochemical assays ( $n \geq 3$ ).

### Isolation of hippocampal subcellular fractions

Mouse hippocampal subcellular fractions were obtained as previously described<sup>6,10</sup>. Hippocampus was extracted, suspended, and lysed in MSH buffer (230 mM mannitol, 70 mM sucrose, 5 mM HEPES, pH 7.4) supplemented with protease and phosphatase inhibitors in a glass homogenizer. The homogenates were centrifuged at  $600 \times g$  for 10 min at 4 °C. The pellet obtained, used for nuclear protein extraction, was resuspended in MSH buffer, homogenized, and then centrifuged at  $600 \times g$  for 10 min at 4 °C. The pellet was resuspended in RIPA buffer and shaken for 30 min at 4 °C. Protein samples were centrifuged at 14,000 rpm for 20 min at 4 °C, and the supernatant obtained corresponds to nuclear proteins. The supernatant fraction obtained at  $600 \times g$  was centrifuged at  $8000 \times g$  for 10 min; the pellet obtained corresponded to the mitochondrial-enriched fraction, and the supernatant obtained corresponded to mitochondria-free cytoplasm. Protein concentration was determined using the BCA kit (Thermo Fisher Scientific, USA).

### Epigenetic and methylation analyses

#### *In silico prediction of CpG islands in the Lonp1 gene*

Using the genomic sequence of chromosome 17 of *Mus musculus*, we extracted the nucleotide sequence for the genomic region comprising 3000 bp downstream and 1000 bp upstream of the Transcriptional Start Site (TSS) for the *Lonp1* gene. The genomic sequence of *Lonp1* was downloaded from GenBank (NC\_000083.7; *Mus musculus* strain C57BL/6 J chromosome 17, GRCm39; region 56,932,873–56,936,873). From this, we predicted the presence of CpG islands using five different methods: 1) Gardiner-Garden (1987) in the Julia Programming Language (versión 1.9.4, JuliaLang, <https://julia-lang.org/>)<sup>42</sup>, 2) Methyl Primer Express (Version 1.0, <https://www.thermofisher.com/order/catalog/product/cl/es/4376041>)<sup>43</sup>, 3) MethPrimer<sup>44</sup> (version 1.1, <https://methprimer.com/cgi-bin/methprimer/methprimer.cgi>), 4) EMBOSS CpGplot (version EMBOSS:6.6.0.0, <https://emboss.sourceforge.net/apps/cvs/emboss/apps/cpgplot.html>)<sup>45</sup>, and 5) CpGProD (Version 1.1, Ponger & Mouchiroud, ([https://doua.prabi.fr/software/cpgprod\\_query](https://doua.prabi.fr/software/cpgprod_query))<sup>46</sup>. Subsequently, a visual inspection was performed to identify consensus genomic regions predicted as CpG islands, facilitating the design of MSP-PCR primers for experimental validation.

#### *MSP-PCR primer design*

Using MethPrimer, forward and reverse primers were designed for the two predicted CpG islands, 1 and 2, respectively, at 5- and 10-nucleotide lengths. Quality control of the design primer was done using MFPrimer (version 3.1 (<https://mfprimer3.igenetech.com/spec>)<sup>47</sup>, where we evaluated the formation of homodimers, heterodimers, and hairpins and filtered out all primers that showed the formation of any of these structures. From this, the primers were manually selected based on PCR product size, GC content percentage, and  $T_m$  to maximize both the PCR product size and the coverage of the predicted CpG islands.

#### *Analysis of global methylation patterns by MSP-PCR*

The methylation status of the *Lonp1* gene promoter was evaluated using a methylation-specific PCR (MSP)<sup>47</sup>. Genomic DNA extraction was performed using the GeneJet Genomic DNA Purification Kit (Thermo Fisher Scientific, cat. K0721) according to the manufacturer's instructions. Genomic DNA was then modified with sodium bisulfite using the Epijet bisulfite conversion kit (Thermo Fisher Scientific, cat K1461), followed by methylation-specific polymerase chain reaction (MSP-PCR) using a Gotaq G2 green master mix kit (Promega, cat M7823). For MSP-PCR, Methylation- or no-methylation-specific primers were designed using the Methprimer bioinformatics software<sup>44</sup>. PCR products were visualized using electrophoresis performed on 2.5% agarose gels. The methylation ratio was obtained by comparing the MSP-PCR product densitometry with the generated partitions to identify differences in methylation levels in the identified CpG islands.

Gene	Forward primer	Reverse primer
<i>Lonp1</i> Methylation	5'- GTAGGAATTGGGAGGGGTTACGT -3'	5'- AATATATAATCCGAATAAAAAACGCT -3'
<i>Lonp1</i> Non-Methylation	5' TTGTAGGAATTGGGAGGGGTTATGT 3'	5' ATATATAATCCAAATAAAAAACACT 3'

#### *Dot blot 5-methylcytosine assay in hippocampal genomic DNA*

Dot Blot DNA assessed the 5-methylcytosine status of genomic DNA from the hippocampus following the manufacturer's instructions<sup>48</sup>. Briefly, genomic DNA was fragmented by sonication using the Bioruptor@ Pico (Diagenode) for ten cycles of 30-s each, with 30 s between cycles. 250 ng fragmented genomic DNA was

denatured in DNA denaturation buffer (200 mM NaOH, 20 mM EDTA) and incubated at 95 °C for 10 min. Then, sodium citrate saline buffer (3.0 M NaCl, 0.3 M Sodium Citrate, pH 7.0) was added and incubated at 4 °C for 5 min. Samples were loaded onto PVDF membranes in a 32-well Slot Blot apparatus (Bio-Rad). The PVDF membrane was UV crosslinked at 1200 J/m<sup>2</sup>. The membrane was blocked in 5% milk in TBS-Tween and incubated with a 5-methylcytosine primary antibody, then with an anti-rabbit IgG peroxidase-conjugated secondary antibody, and finally visualized using an ECL Kit (Luminata Forte Western HRP substrate, Merck Millipore, USA).

### Mecp2 binding analyses

#### *In silico prediction of Mecp2 binding*

We used the same sequence used for CpG island prediction in the *Lonp1* gene. The position weight matrices (PWM) of two known mouse MeCP2 binding motifs were downloaded from the Cis-BP database (<https://cisb.p.cbr.utoronto.ca/>)<sup>49</sup>. The motifs (Cis-BP IDs: Mecp2\_M00806\_2.00, Mecp2\_M09259\_2.00) were transformed into MEME format ((MEME Suite Team, <https://meme-suite.org/>) and then used to scan the *Lonp1* sequence with the FIMO program from the MEME Suite (version 5.5.5, included in MEME Suite Team, <https://meme-suite.org/>)<sup>50</sup>. Significant matches were defined as p-value < 1e-4. The p-value of a motif occurrence is defined as the probability that a random sequence of the same length as the motif matches that position in the sequence with an equal or better score. The q value is also reported as the false discovery rate if the motif occurrence is accepted as significant<sup>50</sup>. Sequence logos were generated from the PWM with ceqlogo of the MEME suite (meme\_v4.11.4, [https://web.mit.edu/meme\\_v4.11.4/share/doc/ceqlogo.html](https://web.mit.edu/meme_v4.11.4/share/doc/ceqlogo.html))<sup>51</sup>. The line plot of p-value and the position was created with Prism 9 (GraphPad Software, Boston, MA, USA).

#### *ChIP-Mecp2 in the mouse hippocampus*

Chromatin immunoprecipitation assay for Mecp2 binding at the *Lonp1* promoter was performed using the EpiQuik Chromatin Immunoprecipitation kit (Epigentek, cat P-2003) on hippocampal tissue from 2- and 7-month-old mice. Hippocampus was disaggregated and crosslinked in 1% formaldehyde for 10 min. After washing off the formaldehyde, hippocampal homogenates were briefly lysed in SDS-containing buffer, followed by sonication for ten cycles of 30 s each to shear genomic DNA using a Bioruptor Pico (Diagenode). DNA fragments were evaluated by agarose gel electrophoresis, yielding fragments ranging from 200 to 500 bp. Subsequently, the DNA-Protein complexes were precipitated with 2 µg of anti-Mecp2 antibody (Abcam, ab2828). DNA was obtained using the EpiQuik Chromatin Immunoprecipitation kit (Epigentek, cat P-2003), following the manufacturer's instructions. The binding of Mecp2 to the *Lonp1* promoter was assessed by real-time PCR from the immunoprecipitated DNA (KAPA SYBR® FAST Master Mix (2X) Kit. Cat: KK4600)<sup>52</sup>.

### Gene expression analysis by quantitative real-time PCR

Total RNA was isolated from the whole hippocampus and the samples were homogenized in Trizol according to the manufacturer's instructions. Total RNA was precipitated and treated with Turbo DNase I (Thermo Fisher Scientific, formerly Invitrogen). Five micrograms of total RNA were reverse transcribed using random hexamers and Oligo d(T)18 and the Super-Script IV reverse transcriptase kit (Invitrogen). The cDNA was quantified by qPCR using specific primers and Kapa SYBR Fast (Kapa Biosystems). The qPCR analysis was performed in duplicate from a reverse-transcribed product using the Rotor-Gene Q (Qiagen). Expression changes were calculated using the 2<sup>-ΔΔCt</sup> method, with cyclophilin-A (*Cyc*) as a normalization control<sup>10</sup>. For the expression of the three *Lonp1* splicing variants, we performed Reverse-Transcriptase-PCR (RT-PCR) using primers flanking exon 1 and conventional RT-PCR using the GoTaq G2 Green Master Mix kit (Promega, cat. M7823).

Gene	Forward primer	Reverse primer
<i>Lonp1</i>	5'- CCGTCAGTATGGCTGTCCA -3'	5'- GAAGACGCCAACATAGGGCT -3'
<i>Lonp1 Exon 1-2</i>	5' CGGTGCGCCGTCAGTAT 3'	5'- AGGAAGACGCCAACATAGGG -3'
<i>Lonp1 Exon 1-2</i>	5'- CTATGGCGGCGAGCACTG -3'	5'- TGGGCGAGACGAACTTTCC -3'
<i>Cyc</i>	5'- GGCAATGCTGGACCAACACAA -3'	5'- GTAAAATGCCCGCAAGTCAAAG-3'

### Protein analyses

#### *Immunoblotting*

The hippocampus from 2- and 7-month-old mice was dissected on ice and immediately processed as previously described<sup>6,10</sup>. Briefly, hippocampal tissue was homogenized in HEPES buffer (25 mM HEPES, 125 mM NaCl, 25 mM NaF, 1 mM EDTA, 1 mM EGTA, 1% NP-40, pH = 7.4) supplemented with a mixture of protease inhibitors (catalog number 78429, Thermo Fisher Scientific) and phosphatase inhibitors (NaF 25 mM, Na<sub>2</sub>P<sub>2</sub>O<sub>7</sub> 30 µM, Na<sub>3</sub>VO<sub>4</sub> 100 mM) using a homogenizer and then passed sequentially through syringes of different gauges. The protein samples were centrifuged at 14,000 rpm for 20 min at 4 °C. Protein concentrations were determined using the BCA protein assay kit (catalog number 23225, Pierce, Rockford, IL, USA). Samples were resolved by SDS-PAGE, followed by immunoblotting on polyvinylidene difluoride (PVDF) membranes. Membranes were incubated with the primary antibody and peroxidase-conjugated mouse or rabbit IgG antibodies (Pierce) and visualized with an ECL kit (Luminata Forte Western HRP substrate, Millipore).

#### *Pharmacological treatment of hippocampal slices*

The brains of 7-month-old SAMP8 mice were dissected and immediately mounted to prepare 350 µm hippocampal slices as previously described<sup>53</sup>. Coronal slices of the whole hippocampus were obtained using

a chopper in a cold, oxygen-saturated cutting solution. The slices were incubated and maintained in artificial cerebrospinal fluid (ACSF, in mM: 124 NaCl, 2.6 NaHCO<sub>3</sub>, 10 D-glucose, 2.69 KCl, 1.25 KH<sub>2</sub>PO<sub>4</sub>, 2.5 CaCl<sub>2</sub>, 1.3 MgSO<sub>4</sub>, 2.60 NaHPO<sub>4</sub>) for one hour. Hippocampal slices were then treated in ACSF as a vehicle for the following treatments: cycloheximide (75 µg/mL) to inhibit protein synthesis for 4 and 6 h, MG132 (20 µM) to inhibit the proteasome for 4 h, and chloroquine (60 µM) to inhibit lysosomes for 5 h. During dissection, cutting, and experimentation, the slices were oxygenated in 95% O<sub>2</sub> and 5% CO<sub>2</sub>. For the proteasomal activity assay, ex vivo hippocampal slices from 3-month-old mice were incubated for 4 h with vehicle or MG132 (20 µM). Proteasomal activity was determined using a fluorogenic substrate conjugated to a proteasome-specific sequence, which emits green fluorescence upon proteolytic cleavage. Cell lysates were prepared in HEPES buffer (HEPES pH 7.4, 0.5 M NaCl, 1 mM EDTA, 1 mM EGTA, 1% NP-40, and 25 mM NaF) supplemented with protease and phosphatase inhibitors. Total protein extracts were quantified, and reactions were conducted in black 96-well microplates (triplicated for each condition) containing 100 µl of assay buffer supplemented with Proteasome Substrate III at a concentration of 5 µl/ml, and 20 µl of sample. The plate was incubated at 37 °C for one hour. Fluorescence intensity was measured using a BioTek microplate reader with excitation/emission at 360/460 nm. The fluorescence obtained is proportional to proteasome activity. Data were collected and normalized to the total protein concentration in each sample for comparative analysis. Results were expressed as a percentage of activity relative to vehicle-treated controls.

### Mitochondrial function assays: ATP production and mitochondrial membrane potential

To stimulate the activity of the ETC complexes, isolated mitochondrial-enriched fractions from the hippocampus of 2 and 7 month-old SAMP8 mice were resuspended in KCl Respiration Buffer (125 mM KCl, 20 mM HEPES, 2 mM MgCl<sub>2</sub>, 2.5 mM KH<sub>2</sub>PO<sub>4</sub>, 0.1% BSA, pH=7.2), with 5 mM pyruvate and 2.5 mM malate as oxidative substrates and incubated at 37 °C for 30 min. For ATP production, 25 µg of mitochondria were incubated with oxidative substrates in a KCl Respiration Buffer for 30 min at 37 °C, then centrifuged at 8000 g for 10 min at 4 °C. The ATP concentration was measured in the supernatant using the luciferin/luciferase bioluminescence assay kit (ATP determination kit no. A22066, Molecular Probes, Invitrogen). The amount of ATP in each sample was normalized to the total protein concentration. Mitochondrial membrane potential was measured in a mitochondrial-enriched fraction (50 µg) diluted in 100 µL of KCl respiration buffer and incubated at 37 °C for 30 min with MitoTracker Red CM-H2Xros. Samples were centrifuged, and the fluorescence was measured at 590 nm in the resuspended mitochondrial pellet.

### Statistical analysis

The results are presented as bar graphs indicating the mean ± SEM, with individual points representing independent biological replicates. Normality was assessed using the Shapiro–Wilk test (GraphPad Prism, GraphPad Software, Inc., La Jolla, CA, USA; Prism software version 8, <https://www.graphpad.com/>). When data were normally distributed, comparisons between two groups were performed using two-tailed unpaired Student's t-tests. In cases where normality was not initially met, a logarithmic transformation ( $Y = \log[Y]$ ) was applied, and normality was re-evaluated. If normality was then confirmed, parametric t-tests were used. Statistical significance was defined as a p-value of ≤ 0.05. For experiments involving four groups, data were tested for normality and analyzed using one-way ANOVA followed by Bonferroni's post hoc test to compare all groups. Statistical significance was defined as a p-value of ≤ 0.05. In the figures, p-values between 0.01 and 0.05 are indicated with one asterisk (\*), values between 0.001 and 0.01 with two asterisks (\*\*), and values < 0.001 with three asterisks (\*\*\*)

### Reagents and antibodies

The following reagents and antibodies were used: Cycloheximide (CAS 66–81-9, Sigma Aldrich), Chloroquine diphosphate salt (C6628, Sigma Aldrich), MG132 (ab141003, Abcam), MSH buffer (230 mM Mannitol, 70 mM sucrose, 5 mM HEPES, 1 mM EDTA, pH=7.4) supplemented with phosphatase (NaF 25 mM, Na<sub>2</sub>P<sub>2</sub>O<sub>7</sub>, 30 µM, Na<sub>3</sub>VO<sub>4</sub> 100 mM) and protease (catalog number 78429, Thermo Fisher Scientific) inhibitors, Saline Sodium Citrate (SSC) Buffer (3 M NaCl, 0.3 M Sodium Citrate, pH=7.0), DNA Denaturing Buffer (200 mM NaOH, 20 mM EDTA), BCA Protein Assay Kit (23,227, Thermo Fisher Scientific). The primary antibodies used were mouse anti-Actin (1:1000, sc-1616, Santa Cruz Biotechnology, Inc), rabbit anti-VDAC (1:1000, sc-390996, Santa Cruz Biotechnology, Inc), rabbit anti-GAPDH (1:1000, sc-25778, Santa Cruz Biotechnology, Inc.), rabbit anti-Lamin A (1:1000, sc-20680, Santa Cruz Biotechnology, Inc.), rabbit anti-Lamin B1 (1:1000, sc-365962, Santa Cruz Biotechnology, Inc.), rabbit anti-Lonp1 (1:1000, PA551692, Termofisher Scientific), rabbit anti-Mecp2 (ab2828, Abcam), rabbit anti-Mecp2 (1:1000, 07–013, Merck Millipore), rabbit anti-Mecp2pSer80 (1:1000, AB2793344, Active Motif), rabbit anti-Mecp2 pSer421 (1:1000, AB254050, Active Motif), rabbit anti-5-Methylcytosine (5-mC) (1:1000, D3S2Z, Cell signaling Technology), mouse anti-β catenin (1:1000, sc-133240, Santa Cruz Biotechnology, Inc.), rabbit anti-LC3B (D11) (1:1000, 3868, cell signaling Technology), rabbit anti-QSMT1-p62 (1:1000, 5114, cell signaling Technology).

## Results

### The *Lonp1* gene contains CpG islands, and its methylation state increases in the hippocampus of aged SAMP8 mice

Changes in DNA methylation patterns in aging occur in multiple tissues, including the brain, thereby allowing the regulation of nuclear gene expression that encodes mitochondrial proteases crucial for mitochondrial function<sup>40,54</sup>. The mitochondrial protease Lonp1 is essential for maintaining the mitochondrial proteome and clearing unfolded or damaged proteins within the mitochondrial matrix<sup>14,55</sup>. DNA methylation studies in human cells have identified changes in methylation at CpG sites in the promoter and regulatory region of the *LONP1*

gene under pathological or environmental conditions, suggesting that its expression is regulated by CpG island methylation<sup>37,38,56</sup>. To determine whether the mouse *Lonp1* gene has putative CpG islands, we searched for them in the promoter region and 5' untranslated region (5' UTR) of the *Lonp1* gene in the *Mus musculus* genome. For this, we employed a combination of two classical rules and CpG island prediction programs, including MethPrimer and Methyl Primer Express, which identified regions of size exceeding 100 base pairs (bp) with a GC percentage above 50% and an observed/expected CpG ratio greater than 60%. Additionally, we utilized three standard CpG island prediction models: Emboss CpG plot, CpGProD, and Gardiner-Garner, all of which identified the region as having a size within the range of 200 to 500 bp, a GC percentage between 60 and 65%, and an observed/expected CpG ratio between 60 and 65%.

In total, four CpG islands were predicted (predicted islands) within this genomic region. Of all these, two CpG islands are closest to the Transcriptional Start Site (TSS), measuring 129 bp and 774 bp (highlighted in light blue, Fig. 1A), identified between the regions -474 bp and +496 bp relative to the TSS of the *Lonp1* gene, using the bioinformatics programs Methprimer and Methyl Primer Express (Fig. 1A). Therefore, these two CpG islands were considered putative (putative islands) and prioritized for further study, which correspond to: (i) island 1, detected by all methodologies, spanning -277 bp to +496 bp relative to the TSS, and (ii) island 2, identified by three of the five methods, spanning -474 bp to -346 bp (Fig. 1B). Based on this analysis, we identified four conserved islands, two located within this region of interest: (i) putative island 1, detected by all methodologies employed, spanning the region -277 bp to +496 bp, and (ii) putative island 2, identified by three of the five methods employed, covering the region -474 bp to -346 bp (Fig. 1B). These results predict that the *Lonp1* gene may be a target of epigenetic regulation. Then, we focused on these two CpG islands for further study, because DNA methylation (5-methylcytosine, 5mCpG) is enriched in the -400/+400 region relative to the TSS and plays a crucial role in gene regulation<sup>57</sup>.

Aging is associated with decreased overall methylation in gene bodies and intergenic regions, and increased methylation in gene promoter regions<sup>58</sup>. To investigate this, we performed dot blot analysis of 5-methylcytosine using fragmented genomic DNA extracted from mouse hippocampal tissues. For this study, we used two mouse models with the same genetic background and age but differing in their aging phenotype: 1) SAMP8 mice, which exhibit signs of accelerated aging starting at 5 months old (mo), and 2) SAMR1 mice, which display a normal aging phenotype. We observed decreased global methylation in the hippocampus of aged SAMP8 mice (7 mo) compared to adult SAMP8 (2 mo) (Fig. 1C). In addition, to corroborate the predicted DNA methylations (5mCpG), we used sodium bisulfite conversion of genomic DNA and methylation-specific PCR (MSP-PCR). Sodium bisulfite treatment converts unmethylated cytosines to uracil and thymine after the PCR reaction and does not convert methylated-modified cytosines. Then, we used the sodium bisulfite-converted genomic DNA as a template for the MSP-PCR reaction. Using the Methprimer program, we designed primers for MSP-PCR to evaluate global methylation and unmethylation changes in the *Lonp1* promoter (Fig. 1D). We observed a significant global increase in 5mCpG methylation near the Transcriptional Start Site (TSS) in the *Lonp1* promoter of aged SAMP8 mice compared to 2-mo SAMP8 mice (Fig. 1E). These results confirm that dynamic changes in DNA methylation occur in gene regulatory regions during aging, with the *Lonp1* gene also exhibiting alterations in this methylation pattern.

### ***Lonp1* is a target gene of *Mecp2*, and their interaction is reduced in the hippocampus of aged SAMP8 mice**

*Mecp2* protein belongs to a family of methylated DNA-binding proteins and is the most expressed protein of this family in the brain<sup>36,39</sup>. Studies have described *Mecp2* as a regulator of genes involved in bioenergetic function and mitochondrial quality control<sup>40,41</sup>. Previous results demonstrated that increased methylation of cytosine (5mCpG) promotes changes in *Lonp1* expression in the hippocampus. Here, we evaluated whether the methylated DNA reader *Mecp2* regulates *Lonp1* gene expression. We evaluated *Lonp1* mRNA in *Mecp2*-null mice. We observed that *Mecp2* null mice exhibited increased *Lonp1* transcripts compared to wild-type (WT) mice (Figure S1). These results suggest that *Mecp2* may act as a transcriptional repressor of *Lonp1* in a context different than aging; however, there are no studies on the function of *Mecp2* in the transcriptional regulation of mitochondrial genes in the aging hippocampus. To study whether *Mecp2* can bind to the promoter region of *Lonp1*, we employed a bioinformatics approach by analyzing *Mecp2* binding motifs in its target genes, as previously reported<sup>59–61</sup>. The genomic region of the mouse *Lonp1* gene was scanned against two known mouse *Mecp2* binding motifs, depicted as sequence logos. For each motif, significant matches ( $p < 5e-4$ ) were found by FIMO (MEME Suite) close to the TSS, three of which coincided with our putative CpG island 1 (Fig. 2A). These results suggest that *Mecp2* may recognize the *Lonp1* gene.

Finally, to corroborate our findings and confirm *Mecp2* binding to the *Lonp1* promoter, we performed chromatin immunoprecipitation (ChIP) for *Mecp2*, followed by quantitative PCR (qPCR) analysis on hippocampal tissue from SAMR1 and SAMP8 mice. We designed primers to target the promoter and 5' UTR regions for qPCR evaluation (Fig. 2B). In qPCR experiments, input DNA was used as a normalizer for assessing *Mecp2* binding to the promoter and 5' UTR regions of *Lonp1*. A non-specific immunoprecipitation control was performed using an antibody against IgG, and, as a positive control, the *H19* gene, which is regulated by *Mecp2* in a methylation-dependent manner<sup>62</sup> (Figure S2). Interestingly, we observed binding of *Mecp2* to the proximal *Lonp1* promoter in the hippocampus of both SAMR1 and SAMP8 mice (Fig. 2C). To determine whether the binding of *Mecp2* changes during aging, a ChIP-qPCR for the *Lonp1* promoter was assessed in 2- and 7-mo SAMP8 mice. As expected, we observed an approximately tenfold increase in the *Lonp1* promoter amplicon compared to the input (chromatin input used in all conditions) in 2-mo SAMP8 mice (Fig. 2C, right panels). However, *Mecp2* binding to the *Lonp1* promoter was decreased in 7-mo SAMP8 mice (Fig. 2C, right panels). Thus, our results demonstrate for the first time that *Lonp1* is a target gene of *Mecp2*, and that *Mecp2*-dependent regulation is altered during aging, resulting in reduced interaction.

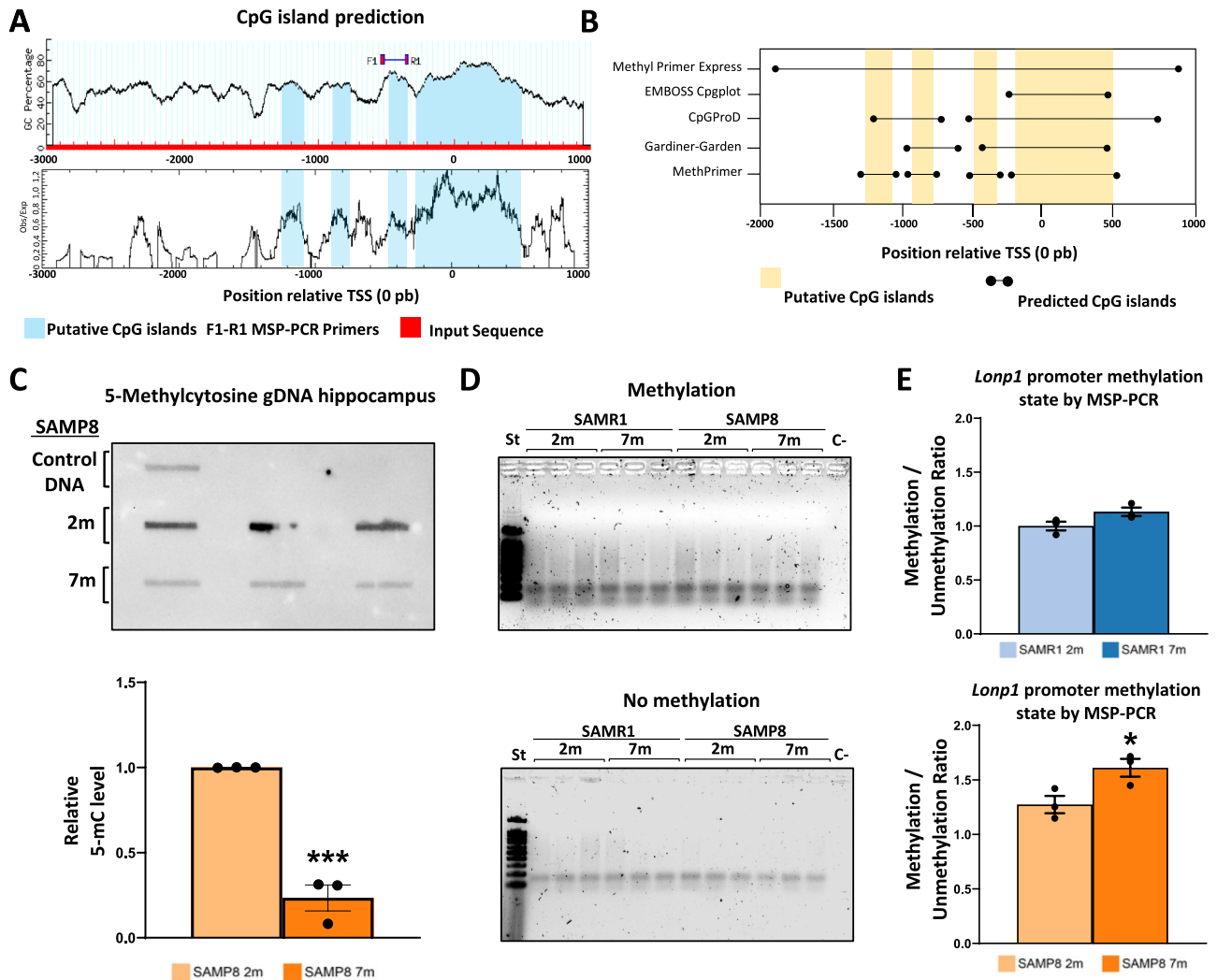


**Fig. 1.** Aging-induced increase in *Lonp1* promoter methylation in the hippocampus of SAMP8 mice. (A) CpG island prediction using MethPrimer and Methyl Primer Express. Four CpG islands were predicted in the promoter and 5' UTR of *Lonp1*, of which two putative islands (129 bp and 774 bp, marked in light blue) were selected for further analysis due to their proximity to the TSS (-474 to +496 bp). (B) CpG islands prediction using Gardiner-Garden (1987) and consensus of putative CpG islands identified near the TSS of *Lonp1* with six bioinformatics programs: MethPrimer, Methyl Primer Express, Takai-Jones, Gardiner-Garden, EMBOSS CpGplot, and CpGProD. Putative islands refer to those prioritized for downstream experimental validation based on consensus and functional relevance. (C) Dot blot analysis and quantification of 5-Methylcytosine (5-mC) from genomic DNA isolated from the hippocampus of 2- and 7-month-old SAMP8 mice. (D) MSP-PCR product is obtained with primers that bind to the oxidation product of methylated CpG and the conversion product of the unmethylated CpGs, the CpG islands (129 bp). (E) Relative quantification of the ratio of densitometry of methylated and unmethylated MSP-PCR products. N = 3 different animals of each age. Graph bars represent means  $\pm$  SEM. \*p < 0.05; \*\*\*p < 0.001.

### Decreased serine 80 phosphorylation of Mecp2 explains its reduced interaction with *Lonp1* promoter in the hippocampus of aged mice

It has been shown that phosphorylation at serine 80 and serine 421 in Mecp2 regulates its binding to target genes. The phosphorylation of Mecp2 is relevant to the expression of genes that promote neuronal activity<sup>63,64</sup>. Specifically, phosphorylation at serine 80 in Mecp2 promotes binding to its gene promoters<sup>64</sup>, and phosphorylation at serine 421 dissociates Mecp2 from the promoters of its target genes<sup>65</sup>. Considering that our ChiP assay revealed a reduced binding of Mecp2 to the *Lonp1* promoter in aging, we evaluated Mecp2 protein levels and phosphorylation at serine 80 and 421. We observed no significant differences in protein levels of total Mecp2 or its phosphorylated forms between 2- and 7 mo SAMR1 mice (Fig. 3A and B). Importantly, we observed decreased protein levels of Mecp2 phosphorylated at serine 80, as well as a decrease in the ratio of Mecp2 serine 80 to total Mecp2, in aged SAMP8 mice (Fig. 3A and C). Thus, our results suggest that the decrease in Mecp2 levels and its phosphorylation at serine 80 could contribute to a reduction in the binding and transcriptional regulation of its target genes, such as *Lonp1*. Therefore, we propose that Mecp2 binds to the

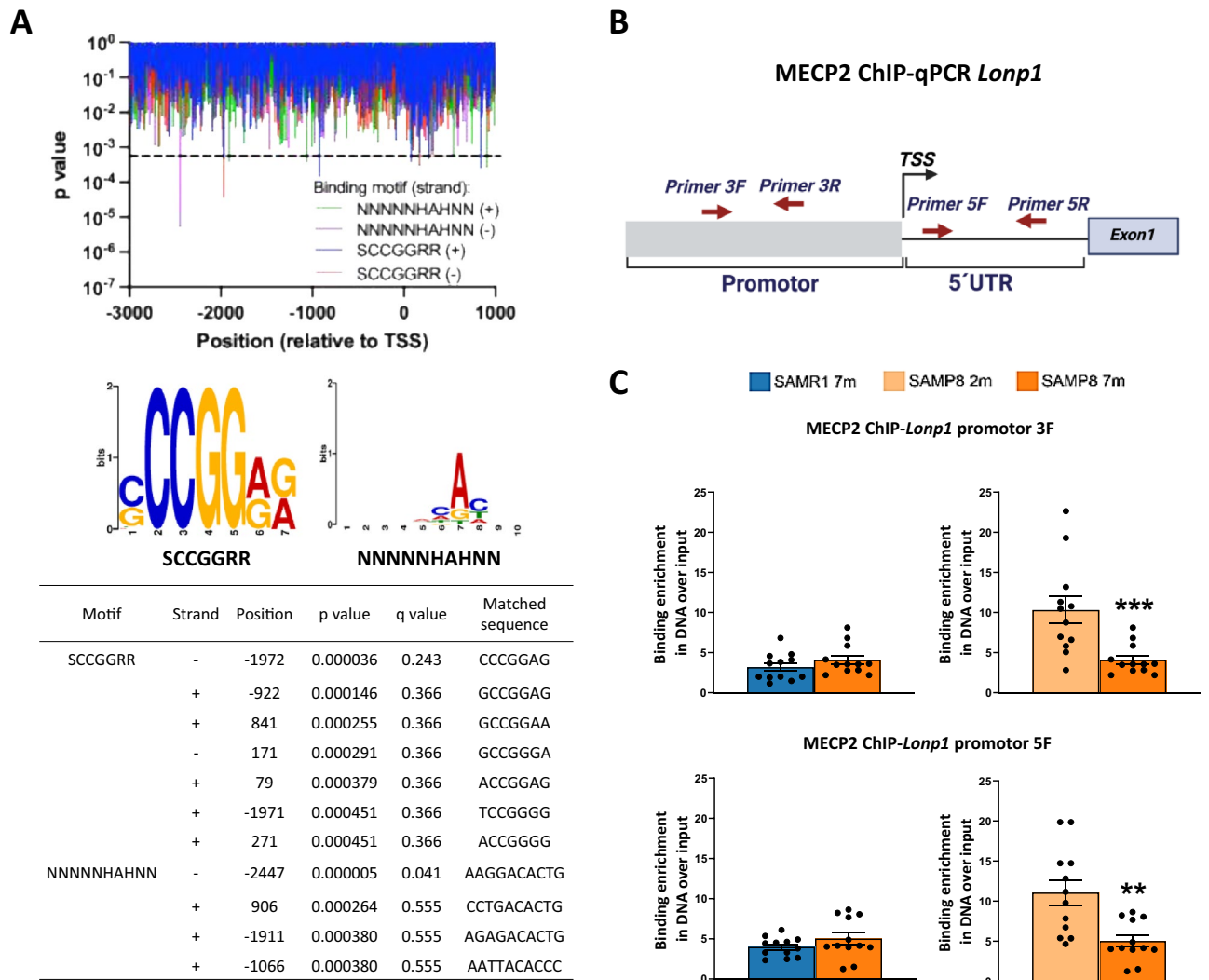


**Fig. 2.** Mecp2 binding at the *Lonp1* promoter mediates the transcriptional upregulation of *Lonp1* in aging mice. **(A)** Prediction of Mecp2 binding sites to the *Lonp1* promoter by position weight matrices (PWM). The sequence of the genomic region of mouse *Lonp1* was scanned against two known mouse Mecp2 binding motifs depicted as sequence logos. For each motif, several significant matches ( $p < 5 \times 10^{-4}$ ) were found by FIMO (MEME Suite). Motif SCCGRR found three hits within putative CpG island 1, spanning the region from -277 to +496 bp relative to the TSS. **(B)** Genetic map of the *Lonp1* gene and alignment of the promoter-targeting primers and 5'UTR to assess the binding of Mecp2 to the *Lonp1* gene. **(C)** Chromatin immunoprecipitation using the anti-Mecp2 antibody. Eluted ChIP-Mecp2 DNA was evaluated with primers at the promoter and 5'UTR of *Lonp1*. ChIP analysis of Mecp2 by qPCR quantification of the 3F promoter of *Lonp1* in the hippocampus of 2- and 7-month-old SAMR1 and SAMP8 mice. ChIP analysis of Mecp2 by qPCR quantification of the 5F 5'UTR of *Lonp1* in the hippocampus of 2- and 7-month-old SAMR1 and SAMP8 mice. ChIP analysis of Mecp2 by qPCR quantification of the 5F promoter of *Lonp1* in the hippocampus of 2- and 7-month-old SAMR1 and SAMP8 mice.  $N = 3$  different animals of each age. Graph bars represent means  $\pm$  SEM. \* $p < 0.05$ . \*\* $p < 0.01$ ; \*\*\* $p < 0.001$ .

*Lonp1* promoter, regulating its expression, and that this modulation is affected in aging, possibly due to reduced serine 80 phosphorylation, which in turn reduces Mecp2 binding to the *Lonp1* promoter.

### Only *Lonp1* protease mRNA variant 1 is expressed in mice, and the levels of *Lonp1* mRNA are upregulated in the hippocampus of aged SAMP8 mice

The nuclear *Lonp1* gene encodes the *Lonp1* protease. In humans, studies have identified three messenger RNA (mRNA) variants of *LONP1*, which are generated through the alternative splicing of exon 1<sup>14,66</sup>. We evaluated whether the three mRNA variants are present in 2- and 7-mo SAMR1 and SAMP8 mice. A primer design flanking exon 1 was performed (Fig. 4A), and the primer design was confirmed using the human duodenal and ovarian cancer cell lines A2780, for which the three *LONP1* mRNA variants have been reported<sup>66</sup>. We observed the three mRNA variants and increased expression of *LONP1* in cancer cells compared with normal

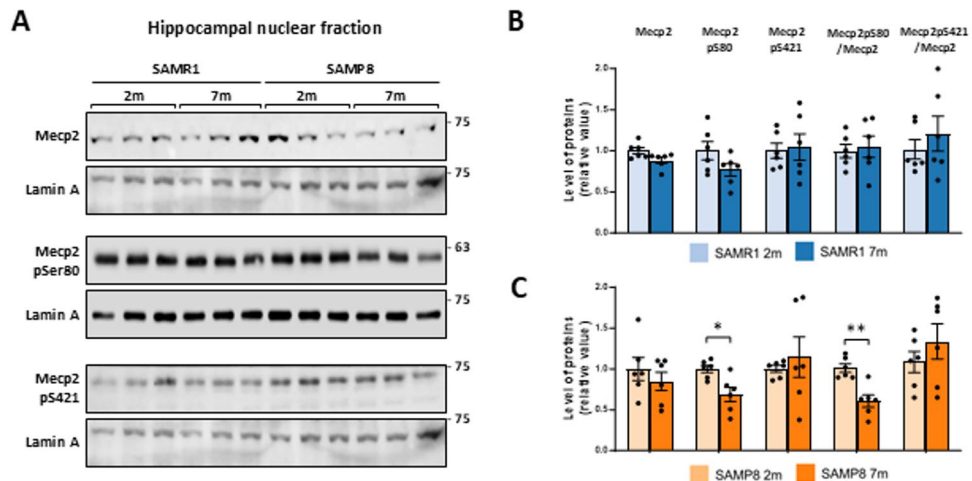


**Fig. 3.** Phosphorylation of Mecp2 at serine 80, which regulates its binding to target genes, is reduced in the hippocampus of aged SAMP8 mice. **(A)** Western blot to identify protein levels of Mecp2, Mecp2 serine 80, and Mecp2 serine 421 in a nuclear hippocampal fraction of 2- and 7-month-old SAMR1 and SAMP8 mice. **(B)** Densitometric analysis of total Mecp2, serine 80, and serine 421, normalized by the nuclear marker lamin A as a loading control, and of Mecp2 serine 80 and serine 421 levels normalized to total Mecp2 levels in SAMR1 mice. **(C)** Densitometric analysis of total Mecp2, serine 80, and serine 421, normalized by the nuclear marker lamin A as a loading control, and of Mecp2 serine 80 and serine 421 levels normalized to total Mecp2 levels in SAMP8 mice. N = 6 different animals of each age. Graph bars represent means  $\pm$  SEM. \* $p < 0.05$ . \*\* $p < 0.01$ .

cells (Fig. 4B), which agrees with previous reports<sup>67,68</sup>. We then evaluated the presence of the three variants in the hippocampal tissue of mice, and interestingly, we only observed the presence of *Lonp1* mRNA variant 1 in the hippocampus of 2- and 7-mo SAMR1 and SAMP8 mice, which corresponds to the mRNA variant without alternative splicing that encodes the full-length isoform of Lonp1 (Fig. 4C). We did not identify mRNA variants 2 and 3 of *Lonp1* in the hippocampus of SAMR1 and SAMP8 mice. Then, we evaluated the kidney, bladder, and lung tissues, which are enriched in mitochondria and have high energy demands to perform their functions<sup>15</sup>. We corroborated only the presence of *Lonp1* mRNA variant 1 in mice using this experimental strategy (Fig. 4D).

Additionally, mRNA levels were analyzed using RT-qPCR. We observed an increase in *Lonp1* mRNA in 7-mo aged SAMP8 mice compared to 2-mo SAMP8 mice (Fig. 4E). These results demonstrate that the *Lonp1* mRNA variant 1 is present in mice, encodes the full-length protein without undergoing alternative splicing, and that its mRNA levels increase in aged SAMP8. In agreement, these results suggest that increased *Lonp1* mRNA levels in aged SAMP8 mice may result from *Lonp1* DNA methylation changes, reduced protein levels, and decreased Mecp2 binding to the *Lonp1* promoter, indicating that Mecp2 acts as a transcriptional repressor of *Lonp1*.

### Lonp1 protein levels are reduced in hippocampal mitochondria of aged SAMP8 mice

Having described that only Lonp1 isoform 1 is present in mice, we next sought to determine its protein levels, which may be localized in both the cytoplasmic and mitochondrial compartments. Additionally, Zanini et al. described that in human cells, Lonp1 has a targeting sequence to the mitochondria (MTS) and another to the nucleus (NLS), translocating to the nucleus under thermal stress conditions<sup>66</sup>. During the aging process, various types of stresses occur, including oxidative, abnormal protein overload, thermal, and others<sup>8,10</sup>. Here, we assessed Lonp1 protein levels in different hippocampal cell fractions of 2- and 7-mo SAMR1 and SAMP8 mice. We observed a significant decrease in Lonp1 protein levels in both the total lysate and the mitochondria-enriched fraction from hippocampal tissue of aged SAMP8 mice compared to 2-mo SAMP8 mice, with no changes in the cytoplasmic or nuclear fractions (Fig. 5A and C). In the SAMR1 mouse groups, no significant changes in Lonp1 protein levels were observed (Fig. 5A and B). To evaluate whether aging affects mitochondrial function in the hippocampus of SAMP8 mice, we analyzed the mitochondrial membrane potential and ATP production in a mitochondrial-enriched fraction isolated from 2- and 7-month-old SAMP8 animals. As shown in Fig. 5D, mitochondria from 7-month-old SAMP8 mice exhibited a significant reduction in membrane potential compared to 2-month-old controls. Similarly, ATP production was markedly decreased in aged SAMP8 mice relative to adult animals. These findings indicate that hippocampal mitochondria undergo a clear functional decline with age, characterized by impaired bioenergetics and reduced capacity to maintain membrane potential, consistent with the onset of mitochondrial dysfunction during early stages of aging in this model. These results indicate that during aging, Lonp1 protein levels decrease in the mitochondria, suggesting that these reduced levels may impair mitochondrial quality control and contribute to the mitochondrial dysfunction characteristic of aging.

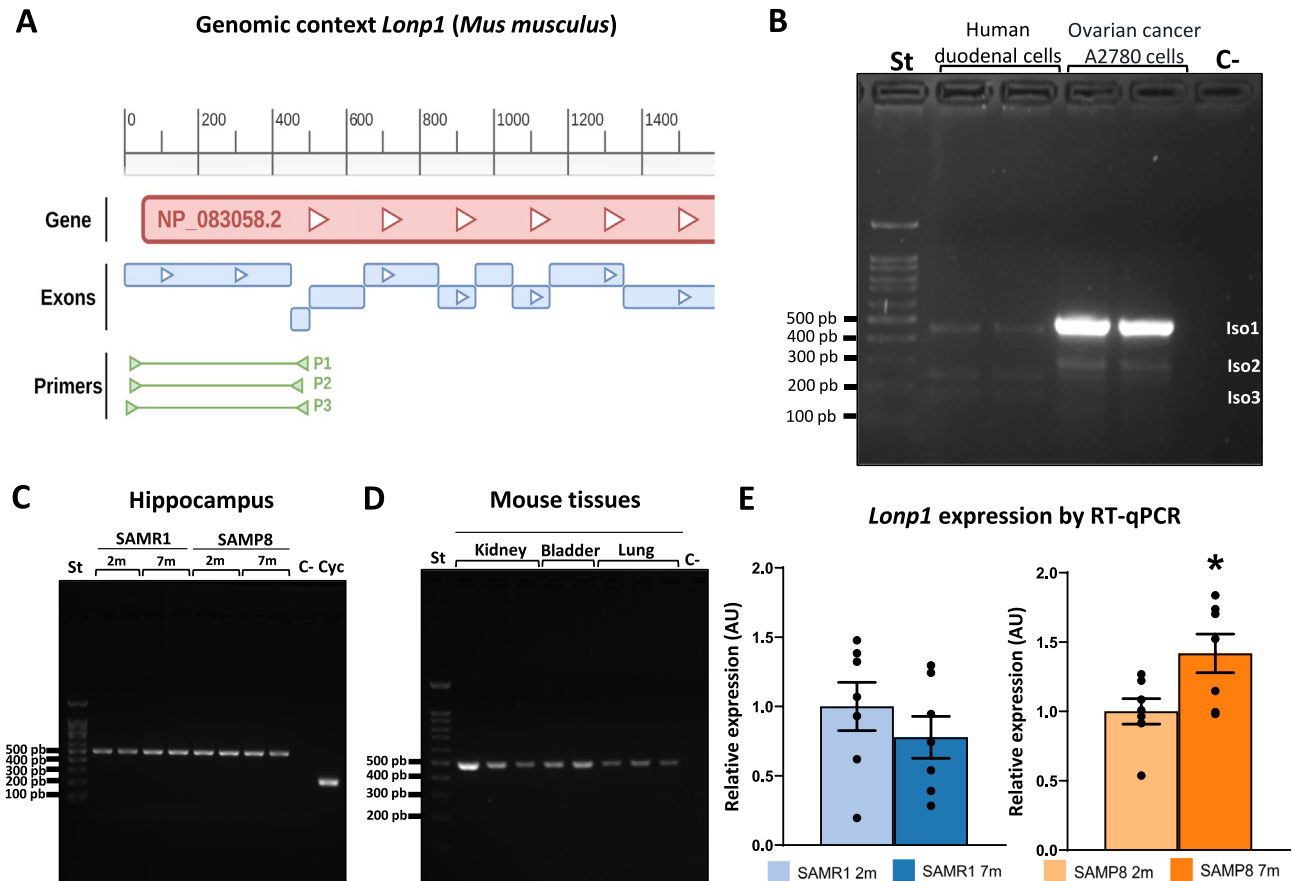


**Fig. 4.** *Lnp1* protease variant 1 is expressed in mouse tissues. **(A)** Gene map of the *Lnp1* gene and alignment of primers flanking exon 1 to assess splicing variants for *Lnp1* mRNA. **(B)** PCR product of the three *Lnp1* mRNA variants in human cells by conventional RT-PCR. **(C)** PCR product of *Lnp1* mRNA variant 1 in the hippocampus of 2- and 7-month-old SAMR1 and SAMP8 mice identified by conventional RT-PCR ( $n=3$ ). **(D)** PCR product of *Lnp1* mRNA variant 1 in kidney, bladder, and lung of 2-month-old SAMR1 mice by conventional RT-PCR. Molecular weight standard of 100 bp. 2% agarose gel. **(E)** Relative quantification of *Lnp1* in the hippocampus of 2- and 7-month-old SAMR1 and SAMP8 mice by RT-qPCR normalized by the  $2^{-\Delta\Delta Ct}$  method using the housekeeping gene Cyclophilin A.  $N=6$  different animals of each age for RT-qPCR and  $N=2$  and 3 for conventional RT-PCR. Graph bars represent means  $\pm$  SEM. \* $p < 0.05$ .

Also, despite the increased *Lnp1* mRNA levels in aging, we observed a paradoxical reduction in *Lnp1* protein levels. This unexpected result suggests a novel regulation of *Lnp1* protein levels that is independent of their epigenetic regulation.

### A lysosomal pathway degrades *Lnp1* protein in aging

Considering that mRNA and protein levels of *Lnp1* are inconsistent, diverse explanations may exist, such as changes in the half-life or increased degradation of de novo synthesized *Lnp1* protein. Using human colorectal cancer cells (SW480), researchers have suggested that both lysosomal and proteasomal pathways can degrade *Lnp1*<sup>67</sup>. However, there is no evidence of in vivo *Lnp1* degradation pathways in mouse cells. To investigate this, we treated ex vivo hippocampal slices from 3-mo mice with the proteasome inhibitor MG132 (Fig. 6A) and the lysosomal inhibitor chloroquine (CQ) (Fig. 6B) to explore potential degradation mechanisms of *Lnp1* that could explain its reduced protein levels in the aged hippocampus. Our findings indicated that treatment with MG132, a reversible inhibitor of proteasome catalytic subunits<sup>69</sup>, did not alter *Lnp1* protein levels in either the cytosolic or mitochondrial fractions (Fig. 6A). To validate the effectiveness of MG132 under our experimental conditions, we additionally measured proteasome activity using a fluorogenic peptide substrate in hippocampal slices from 3-month-old mice. This assay confirmed that MG132 treatment (20  $\mu$ M, 4 h) reduced proteasomal proteolytic activity by  $\sim 78\%$  compared to vehicle-treated controls (Supplementary Fig. 3), thereby supporting the interpretation that *Lnp1* degradation is not mediated by the proteasome. In contrast, treatment with CQ, a weak base that diffuses into the lysosomal membrane and increases lysosomal pH, thereby reducing its activity<sup>70</sup>, led to a significant increase in *Lnp1* levels as well as in p62 and the LC3 II/I ratio (Fig. 6B), indicating that *Lnp1* is primarily degraded via a lysosome-dependent pathway in the hippocampus of aged mice.

Additionally, cycloheximide (CHX) treatment, which is known to inhibit cytoplasmic protein synthesis in human colorectal cancer cells (SW480), has demonstrated that the *Lnp1* protease has a half-life of 6 to 8 h<sup>67</sup>.

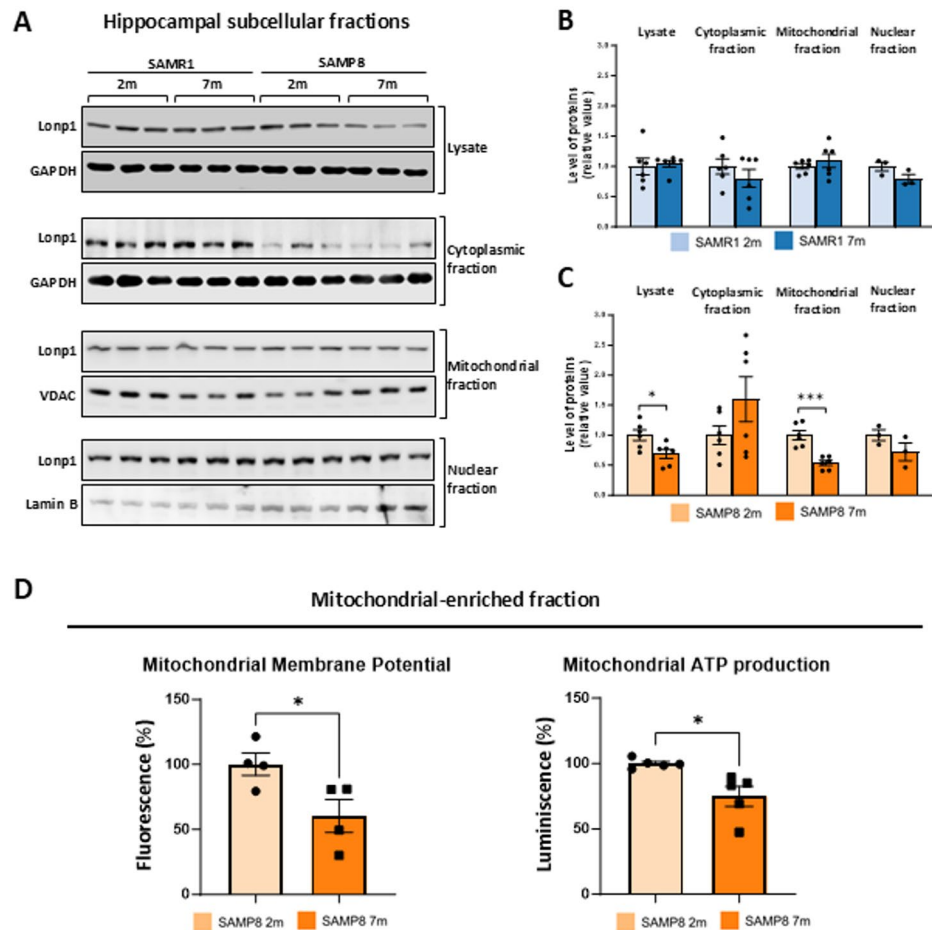


**Fig. 5.** Decreased protein levels of Lonp1 during hippocampal aging of female SAMP8 mice. **(A)** Western blot to identify protein levels of Lonp1 in a total lysate, cytoplasmic fraction, mitochondria-enriched fraction, and nuclear fraction from the hippocampus of 2- and 7-month-old SAMR1 and SAMP8 mice. **(B)** Densitometric analysis of Lonp1 in different subcellular fractions of the hippocampus of 2- and 7-month-old SAMR1 mice, normalized by the expression of loading controls: Total lysate and cytoplasm (GAPDH); Mitochondria (VDAC) and Nuclear (Lamin B). **(C)** Densitometric analysis of Lonp1 levels in the hippocampus of 2- and 7-month-old SAMP8 mice, normalized by their respective loading control. N = 3 for cytoplasmic and nuclear fractions. N = 6 for total lysate and mitochondria-enriched fraction. **(D)** Mitochondrial membrane potential (N = 4 per group) and ATP production (N = 5 per group) in hippocampal mitochondrial-enriched fractions from SAMP8 mice. Graph bars represent means  $\pm$  SEM. \* $p < 0.05$ . \*\* $p < 0.01$ .

Using CHX and CQ in *ex vivo* hippocampal slices from aged SAMP8 mice (7-month-old), we observed a decrease in Lonp1 levels at 6 h of CHX treatment. Interestingly, this degradation is prevented after 6 h of CQ treatment (Fig. 6C). These findings indicate that the primary mechanism of Lonp1 degradation in the mouse hippocampus is lysosomal, with a Lonp1 half-life of more than 6 h. Thus, these results suggest that, despite reduced Mecp2-dependent regulation of Lonp1 leading to increased mRNA levels, Lonp1 protein levels are compromised during aging, likely due to enhanced lysosomal degradation in the hippocampus of aged SAMP8 mice.

In summary, our results demonstrate, for the first time, methylation changes in the Lonp1 promoter in the hippocampus of aged mice. We also reveal that the epigenetic reader Mecp2 transcriptionally represses Lonp1 expression, with reduced binding and phosphorylation at serine 80 of Mecp2, potentially explaining the increased Lonp1 transcript levels. However, despite the increase in Lonp1 mRNA levels, Lonp1 protein levels are diminished in the hippocampus of aged SAMP8 mice, partly due to lysosomal degradation.

## Discussion

The present study sheds new light on the complex interplay between epigenetic regulation and mitochondrial proteostasis in the aging hippocampus. Our findings demonstrate for the first time that the transcriptional regulator Mecp2 binds to the promoter region of Lonp1, a key mitochondrial protease, and that this interaction is diminished in aged SAMP8 mice. This age-associated reduction in Mecp2 binding correlates with increased Lonp1 mRNA levels, suggesting that Mecp2 normally acts as a repressor of Lonp1 transcription in hippocampal

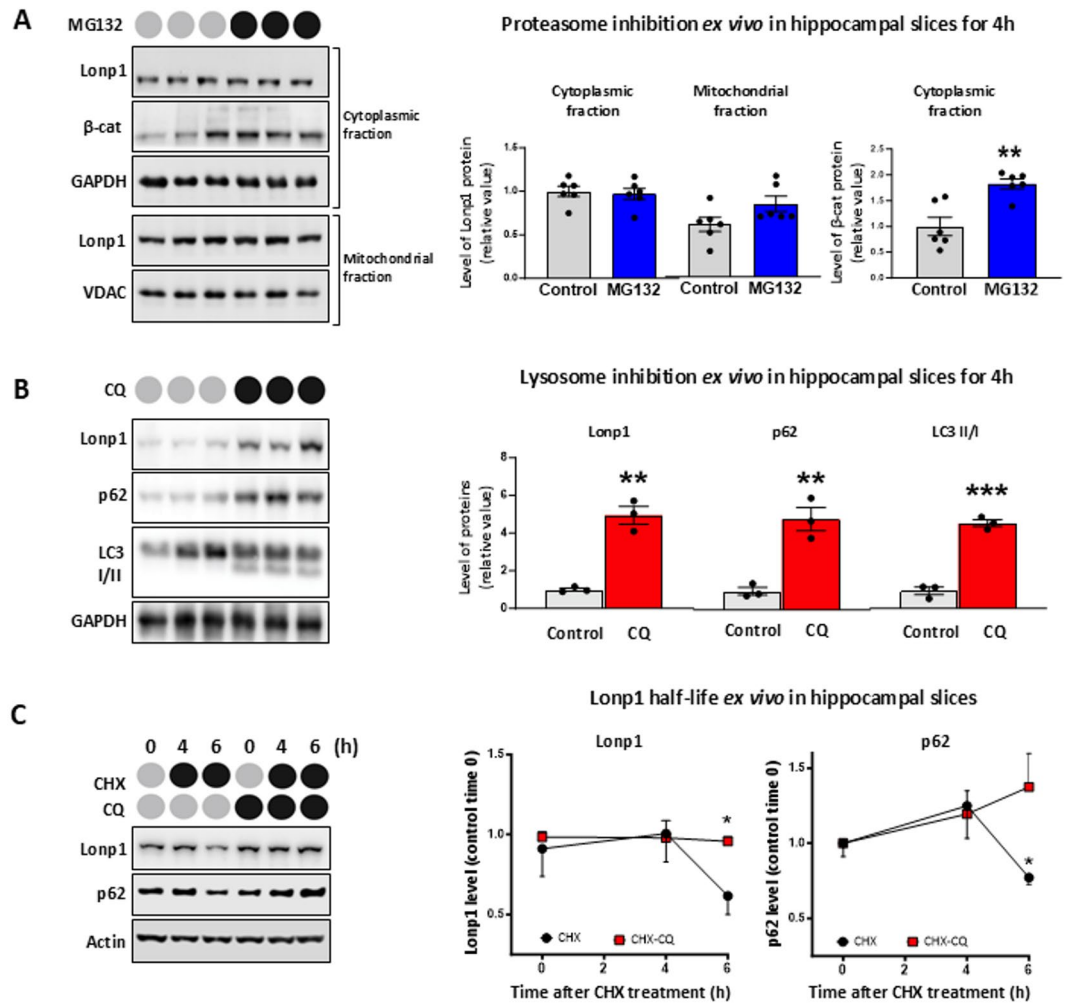


**Fig. 6.** Chloroquine increases Lonp1 accumulation, and its turnover rate is 6 h in the presence of cycloheximide from *ex-vivo* treatment of mouse hippocampal slices. **(A)** Western blot to identify protein levels of Lonp1 and  $\beta$ -catenin in cytoplasmic and mitochondrial fractions from hippocampal slices from 3-month-old mice, treated with the proteasome inhibitor MG132 (20  $\mu$ M) for 4 h. **(B)** Western blot to identify protein levels of Lonp1, p62 and LC3 in a total lysate from hippocampal slices from 3-month-old mice, treated with the inhibitor chloroquine at 60  $\mu$ M for 5 h. **(C)** Western blot to identify protein levels of Lonp1 and p62 in a total lysate from hippocampal slices from aged SAMPM8 mice (7-month-old), treated with the inhibitor chloroquine (60  $\mu$ M) and cycloheximide (75  $\mu$ g/mL) for 0, 4, and 6 h. N = 3 different animals for MG132, chloroquine, and cycloheximide treatments. Graph bars represent means  $\pm$  SEM. \* $p < 0.05$ . \*\* $p < 0.01$ . \*\*\* $p < 0.001$ .

neurons, providing evidence of a novel mechanism for regulating Lonp1 expression. Interestingly, despite this transcriptional upregulation, Lonp1 protein levels are significantly reduced in aged tissue, an effect at least partially explained by degradation through the lysosomal pathway. This disconnect between mRNA and protein abundance highlights the complex and multifaceted nature of mitochondrial quality control in the aging brain (Fig. 7).

Our findings also shed light on the transcriptional regulation of Lonp1. Bioinformatic analyses identified four CpG islands within the Lonp1 promoter region (−474 to +496 bp relative to the TSS reference in *Mus musculus*), including a CpG island spanning the TSS (−400 to +400 bp), a region typically involved in methylation-dependent gene regulation<sup>57</sup>. We observed increased local methylation within the Lonp1 promoter in aged hippocampal tissue, even as global DNA methylation (5-mC) decreased—a pattern previously reported in the aging brain and thought to contribute to transcriptional dysregulation<sup>71</sup>. Increased methylation in gene promoter regions has been reported in aged individuals, likely due to the decreased expression of epigenome writers and DNA methyltransferases<sup>58</sup>. The LONP1 gene has been previously shown to change its methylation pattern. For example, humans exhibit methylations in regulatory regions that modulate their expression in patients exposed to environmental contamination and myalgic encephalomyelitis syndrome<sup>37,38,72</sup>. A limitation of our study is the absence of internal loading controls in the methylation and dot blot assays (Fig. 1C and D).

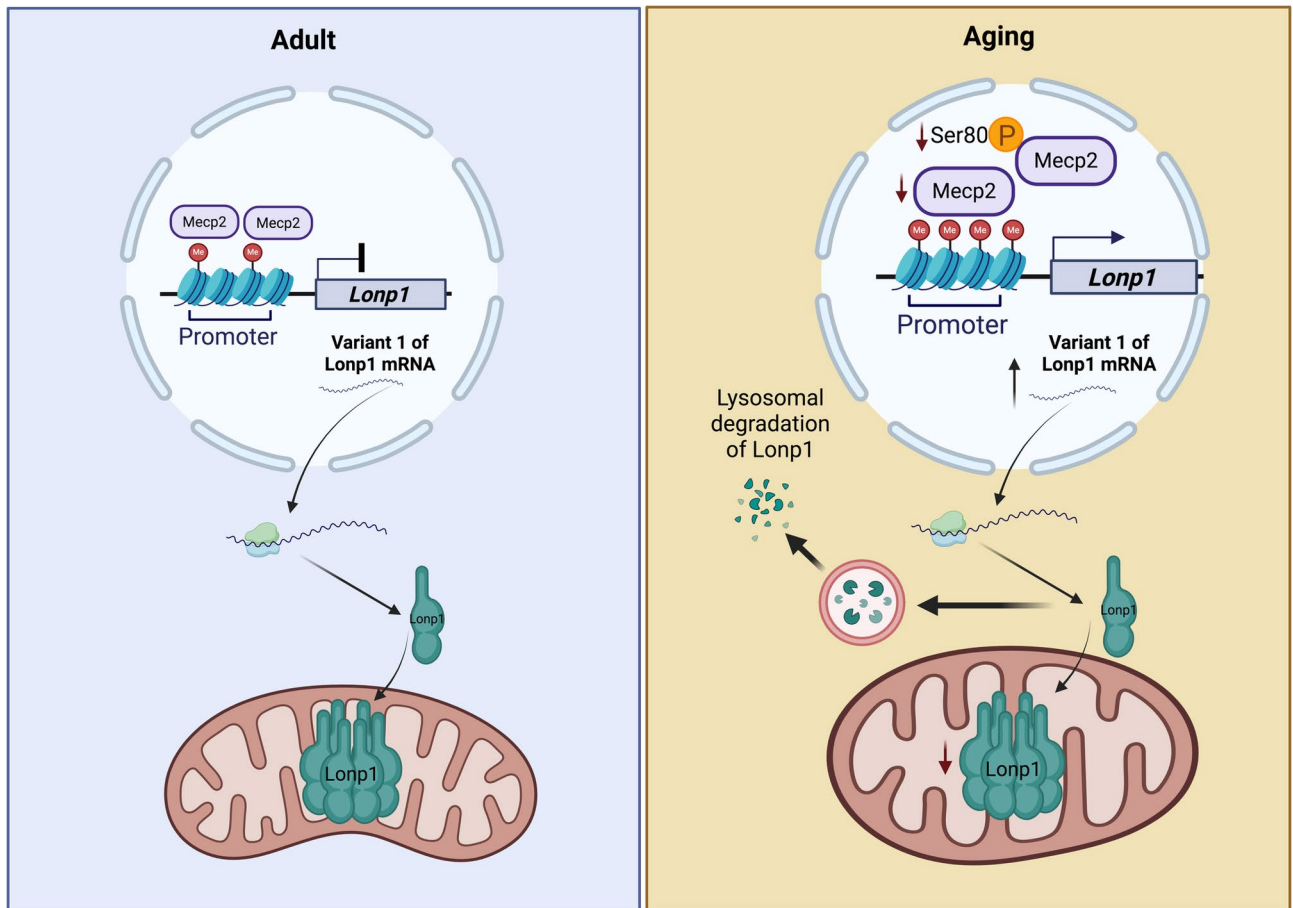


**Fig. 7.** Scheme summarizing findings on Mecp2-mediated regulation of Lonp1 in the aged hippocampus. This study demonstrates that Mecp2 functions as a transcriptional repressor of Lonp1 by binding to CpG-rich regions located near its promoter. In aged mice, Mecp2 binding is reduced, correlating with increased Lonp1 mRNA levels. Unlike humans, mice express only the full-length mitochondrial Lonp1 isoform. However, despite this transcriptional upregulation, Lonp1 protein levels are decreased, possibly due to lysosomal degradation. These findings reveal a novel mechanism linking epigenetic regulation and protein degradation pathways in the control of mitochondrial proteostasis during aging, highlighting Mecp2 and Lonp1 as potential therapeutic targets in age-related cognitive decline.

Although these results consistently show increased DNA methylation in aged hippocampal tissue, future studies incorporating appropriate loading controls will be essential to further validate and strengthen these findings.

The CpG sites can be methylated, hydroxymethylated, or free of methylation. The state of CpG methylation can affect the binding affinity of methyl-binding domain (MBD) proteins, such as Mecp2, which may act as transcriptional repressors or activators depending on the context<sup>73,74</sup>. Few studies report Mecp2 as a regulator of mitochondrial gene expression.

Previous transcriptional studies in Peripheral Blood Mononuclear Cells (PBMC) from patients with Rett syndrome have reported altered expression of mitochondrial genes essential for bioenergetic structure and function<sup>40</sup>. Additionally, a comprehensive RNA sequencing study was conducted in hippocampal Mecp2 knockdown rats. They observed expression changes in 2 mitochondrial proteases: the serine protease Htra2 and the ATP-dependent protease Clpx. Both soluble proteases, localized in the intermembrane space and mitochondrial matrix, respectively, regulate mitochondrial protein quality control in conjunction with Lonp1<sup>75</sup>. Notably, both Clpx and Lonp1 are located on mouse chromosome 17<sup>55</sup>. Therefore, both genomic and functional proximity could indicate that Mecp2 can regulate the expression of the Lonp1 gene, raising the possibility of coordinated regulation.

We confirmed Mecp2 binding to the Lonp1 promoter through *in silico* predictions using validated Mecp2 binding motifs and ChIP assays. Surprisingly, this binding was reduced in aged SAMP8 mice. This reduction correlates with a decrease in total Mecp2 protein, suggesting that reduced protein levels may lead to a decrease in binding. In addition, the phosphorylation sites on Mecp2 regulate its binding capacity to the promoters of its target genes<sup>64,65</sup>. We also found that phosphorylation at Ser80 is decreased in aged mice, a modification critical for promoting chromatin binding<sup>64</sup>. Although phosphorylation at Ser421 was unchanged, the loss of Ser80 phosphorylation may be sufficient to explain reduced promoter interaction. We derive this idea from mutation studies, where serine 80 was replaced by alanine (S80A), resulting in attenuated binding of Mecp2 to

chromatin and, consequently, decreased expression of its target genes and Mecp2-dependent neuronal activity<sup>64</sup>. Interestingly, phosphorylations at serine 80 and 421 are oppositely regulated<sup>63,64</sup>. Other phosphorylations may also be involved in modulating the function of Mecp2<sup>65</sup>. Further studies are required to delineate Mecp2's phosphorylation-dependent dynamics fully. Collectively, our data support the role of Mecp2 as a transcriptional repressor of Lonp1 for three main reasons: (1) Lonp1 mRNA is elevated in Mecp2 knockout mice; (2) Mecp2 protein and its Ser80-phosphorylated form are reduced in aged SAMP8 mice, coinciding with increased Lonp1 transcript levels; and (3) ChIP assays revealed decreased Mecp2–promoter interaction with aging. Thus, we demonstrated a novel mechanism that regulates Lonp1 gene expression, which may be modulated by factors such as aging.

Interestingly, however, no significant differences in Mecp2 binding were detected when comparing 7-month-old SAMR1 and SAMP8 animals. This finding suggests that the resistance of SAMR1 to accelerated senescence does not involve higher Mecp2 occupancy at the Lonp1 promoter, but rather the operation of alternative regulatory pathways. Such mechanisms, independent of Mecp2 phosphorylation, may include differences in CpG/5-hmC profiles, chromatin accessibility, or co-regulator dynamics, which could maintain Lonp1 expression without requiring increased Mecp2 binding. Thus, while aging in SAMP8 is characterized by a decline in Mecp2–Lonp1 interactions, SAMR1 resilience appears to depend on distinct epigenetic mechanisms. Now, although we demonstrate a novel mechanism of epigenetic regulation of Lonp1 mediated by Mecp2, future studies should incorporate conditional overexpression and *in vivo* rescue approaches to conclusively establish causality in the Mecp2–Lonp1 regulatory axis during aging. Such studies would provide definitive evidence that the reduction in Mecp2 phosphorylation at Ser80 is both necessary and sufficient for the upregulation of the Lonp1 transcript observed during aging.

Regarding Lonp1 transcript diversity, human cells express three isoforms through the alternative splicing of exon 1, which differ in the amino acid sequence of the N-terminal domain<sup>31,76</sup>. These isoforms display distinct subcellular distributions and tissue-dependent expression<sup>66</sup>. Isoform 1 is the canonical mitochondrial variant, mainly localized to the matrix but also detected in the nucleus, where it regulates proteostasis and mitochondrial function<sup>31,76</sup>. Isoform 2, truncated at the N-terminus, shows reduced mitochondrial import and is found in the cytoplasm, nucleus, and mitochondria-associated membranes, where it protects against ER stress in cooperation with TRAP1<sup>77,78</sup>. Isoform 3 lacks exon 1, is fully extramitochondrial and has an unknown function, but under stress relocates to the nucleus, where it may degrade transcription factors such as HSF1, modulating stress-induced programs<sup>31</sup>. The expression of these variants in humans is influenced by cell type, stress, aging, and cancer metabolic reprogramming<sup>31,66</sup>. Using RT-PCR with primers flanking exon 1, we confirmed the presence of three products (482, 210, and 180 bp) in human cells, with altered variant distribution in cancer cells, consistent with previous reports<sup>66</sup>. In contrast, only variant 1, encoding the canonical isoform, was detected in mouse tissues, including hippocampus, kidney, lung, and bladder.

On the other hand, although Lonp1 mRNA levels were elevated in aged SAMP8 mice, protein levels were reduced. We observed that Lonp1 protease decreases its protein levels in the whole hippocampal lysate and the mitochondrial fraction of the hippocampus of aged mice. Interestingly, in studies of Lonp1 haploinsufficient mice, decreased Lonp1 expression promotes a structural and bioenergetic loss of mitochondria<sup>15</sup>. Several mechanisms could explain this inverse relationship: (i) compensatory transcriptional upregulation<sup>68</sup>, (ii) impaired translation<sup>79</sup>, (iii) accelerated *de novo* synthesized protein degradation<sup>80</sup>, or (iv) post-transcriptional silencing by microRNAs<sup>81</sup>, although miRNA-mediated regulation of Lonp1 remains unexplored in mice. We demonstrate that Lonp1 protein levels are specifically reduced in mitochondria during aging, without evidence of a significant cytoplasmic accumulation, suggesting that this reduction is unrelated to altered mitochondrial import of the newly synthesized Lonp1 protein.

Reduced protein levels of Lonp1 in aged hippocampal mitochondria may promote a loss of mitochondrial quality control, resulting in compromised mitochondrial proteome integrity. For the first time, we describe that the half-life of the Lonp1 protein in the hippocampus is 6 h. Our data indicate that lysosomal rather than proteasomal degradation accounts for the reduction in Lonp1 protein levels. This conclusion is supported by experiments in hippocampal slices treated with MG132, where the abundance of Lonp1 protein remained unchanged. Importantly, at the concentration used (20  $\mu$ M), MG132 has been demonstrated to effectively inhibit proteasome catalytic subunits without directly affecting Lonp1 activity<sup>69,82</sup>. Consistently, our proteasome activity assay using a fluorogenic peptide substrate confirmed a 78% reduction in proteasomal activity following MG132 treatment, validating the effectiveness of the inhibition under our experimental conditions (Supplementary Fig. 3). Nevertheless, we acknowledge that complementary approaches, including autophagy inhibition or ubiquitination assays, will be necessary to fully exclude alternative degradation pathways contributing to Lonp1 regulation. More importantly, lysosomal inhibition in the absence of *de novo* protein synthesis restored Lonp1 protein levels, indicating this pathway as the primary route for its degradation in hippocampal tissue. This also suggests that the *de novo* protein synthesis of Lonp1 is degraded by a route involving the lysosome, which limits the availability of Lonp1 protein in the mitochondria during aging. This finding aligns with a recent study showing that deacetylation of Lonp1 at lysine 145 by SIRT3 promotes its ubiquitination and subsequent degradation<sup>67</sup>. Future studies will investigate the mechanisms involved in the degradation of Lonp1 protein before its mitochondrial import.

Mitochondrial dysfunction is a hallmark of aging, particularly in the hippocampus, where mitochondria, particularly synaptic mitochondria, are highly susceptible to oxidative stress and calcium overload<sup>8</sup>. Lonp1 is a key protease in mitochondrial quality control, maintaining proteostasis and the integrity of the electron transport chain. It specifically supports the remodeling and functionality of the complexes, thereby counteracting the increase of ROS<sup>68,83</sup>. Therefore, reduced levels of Lonp1 protein in the mitochondria could be responsible, at least in part, for the mitochondrial dysfunction of the hippocampus, which ultimately contributes to impaired learning and memory capacities in aging. This is supported by studies in Lonp1 haploinsufficient mice, which

demonstrate a decrease in Lonp1 expression, resulting in a structural and bioenergetic loss of mitochondria<sup>15</sup>. The same effect is observed in studies of Lonp1 silencing in cancer cells, which decreases the stability of mitochondrial complexes and bioenergetics<sup>83,84</sup>.

Additionally, Lonp1 has also been reported to translocate to the nucleus under heat stress, possibly modulating transcription by degrading HSF1 (heat shock factor 1). Furthermore, it has been suggested that Lonp1 has a nuclear localization signal (NLS) and relocalizes from the mitochondria to the nucleus in human cells<sup>31</sup>. Here, we confirmed nuclear localization of Lonp1 in the hippocampus of both adult and aged mice, without significant age-related changes, suggesting a constitutive presence in this compartment under non-stress conditions. More studies are necessary to understand other functions of Lonp1 in the nucleus.

Finally, although Lonp1 transcripts are elevated in aged tissue, protein levels are markedly reduced. This paradox may appear unexpected, but similar patterns have been reported in other systems. For example, in models of synaptic plasticity, transcription of PSD95 (Dlg4) or AMPA receptor subunits can be enhanced despite reduced protein abundance, reflecting compensatory attempts to restore synaptic homeostasis<sup>85,86</sup>. Likewise, increased transcription of proteasome subunits has been described under impaired proteasomal activity, even when protein levels remain diminished<sup>87</sup>. Other well-documented cases include regulatory proteins such as p53, whose mRNA may rise while the protein is kept low due to rapid proteasomal degradation mediated by MDM2<sup>88</sup>, and cyclins, which are transcriptionally induced but tightly controlled by accelerated protein turnover<sup>89</sup>. Together, these examples support the notion that Lonp1 regulation during aging may involve analogous responses coupled to post-transcriptional mechanisms that limit protein abundance. Thus, this may reflect a homeostatic compensatory response, particularly relevant in the Lonp1 regulation.

In summary, our study identifies a novel mechanism of Mecp2-dependent epigenetic regulation of Lonp1, linking transcriptional repression and promoter methylation with protein degradation and mitochondrial dysfunction in the aging brain. These insights lay the groundwork for future therapeutic strategies aimed at preserving mitochondrial quality control in neurodegenerative conditions.

## Conclusions

These findings reveal a novel epigenetic mechanism that regulates Lonp1 expression in the aging hippocampus. The observed DNA methylation changes and altered Mecp2 function suggest a complex regulatory axis controlling Lonp1 transcription. Notably, the dissociation between increased Lonp1 mRNA and reduced protein levels highlights post-transcriptional regulation, including lysosomal degradation, as a critical factor in age-related decline. This evidence also extends previous work on Lonp1 in non-neuronal tissues by demonstrating its transcriptional regulation in neurons and implicating Mecp2, a protein best known for its role in Rett syndrome, as a critical modulator of mitochondrial function during aging. Furthermore, while prior studies have shown that mitochondrial dysfunction is a hallmark of both normal aging and neurodegenerative diseases, our results offer a mechanistic link between age-related epigenetic changes and impaired mitochondrial proteostasis. The identification of Mecp2 and Lonp1 as key players in this pathway suggests potential therapeutic targets for mitigating cognitive decline and neurodegeneration. In particular, strategies aimed at modulating Mecp2 activity or enhancing Lonp1 stability may offer novel avenues for preserving hippocampal function during the aging process.

## Data availability

For all the data supporting the reported results, please contact the corresponding author of the study.

Received: 29 July 2025; Accepted: 15 October 2025

Published online: 19 November 2025

## References

- Jin, M. & Cai, S. Q. Mechanisms Underlying Brain Aging Under Normal and Pathological Conditions. *Neurosci Bull* **39**(2), 303–314 (2023).
- Lopez-Otin, C. et al. Hallmarks of aging: An expanding universe. *Cell* **186**(2), 243–278 (2023).
- Stauch, K. L., Purnell, P. R. & Fox, H. S. Aging synaptic mitochondria exhibit dynamic proteomic changes while maintaining bioenergetic function. *Aging (Albany NY)* **6**(4), 320–334 (2014).
- Wisdom, N. M., Mignogna, J. & Collins, R. L. Variability in Wechsler Adult Intelligence Scale-IV subtest performance across age. *Arch Clin Neuropsychol* **27**(4), 389–397 (2012).
- Lemaitre, H. et al. Normal age-related brain morphometric changes: nonuniformity across cortical thickness, surface area and gray matter volume?. *Neurobiol Aging* **33**(3), 617 (2012) (e1–9).
- Torres, A. K. et al. Pathologically phosphorylated tau at S396/404 (PHF-1) is accumulated inside of hippocampal synaptic mitochondria of aged Wild-type mice. *Sci Rep* **11**(1), 4448 (2021).
- Lasagna-Reeves, C. A. et al. Tau oligomers impair memory and induce synaptic and mitochondrial dysfunction in wild-type mice. *Mol Neurodegener* **6**, 39 (2011).
- Olesen, M. A. et al. Premature synaptic mitochondrial dysfunction in the hippocampus during aging contributes to memory loss. *Redox Biol* **34**, 101558 (2020).
- Picard, M. & McEwen, B. S. Mitochondria impact brain function and cognition. *Proc Natl Acad Sci USA* **111**(1), 7–8 (2014).
- Torres, A. K. et al. Mitochondrial Bioenergetics, Redox Balance, and Calcium Homeostasis Dysfunction with Defective Ultrastructure and Quality Control in the Hippocampus of Aged Female C57BL/6J Mice. *Int. J. Mol. Sci.* **24**(6), 5476 (2023).
- Lores-Arnaiz, S. et al. Brain cortex mitochondrial bioenergetics in synaptosomes and non-synaptic mitochondria during aging. *Neurochem Res* **41**(1–2), 353–363 (2016).
- Glynn, S. E. Multifunctional Mitochondrial AAA Proteases. *Front Mol. Biosci.* **4**, 34 (2017).
- Campello, S., Strappazzon, F. & Ceconi, F. Mitochondrial dismissal in mammals, from protein degradation to mitophagy. *Biochim Biophys Acta* **1837**(4), 451–460 (2014).
- Gibellini, L. et al. The biology of Lonp1: More than a mitochondrial protease. *Int Rev Cell Mol Biol* **354**, 1–61 (2020).
- De Gaetano, A. et al. Impaired Mitochondrial Morphology and Functionality in Lonp1(wt/-) Mice. *J. Clin. Med.* **9**(6), 1783 (2020).

16. Zurita Rendon, O. & Shoubridge, E. A. LONP1 Is Required for Maturation of a Subset of Mitochondrial Proteins, and Its Loss Elicits an Integrated Stress Response. *Mol Cell Biol* **38**(20), e00412–e417 (2018).
17. Ruan, L. et al. Cytosolic proteostasis through importing of misfolded proteins into mitochondria. *Nature* **543**(7645), 443–446 (2017).
18. Rep, M. et al. Promotion of mitochondrial membrane complex assembly by a proteolytically inactive yeast Lon. *Science* **274**(5284), 103–106 (1996).
19. Cheng, C. W. et al. Overexpression of Lon contributes to survival and aggressive phenotype of cancer cells through mitochondrial complex I-mediated generation of reactive oxygen species. *Cell Death Dis.* **4**(6), e681 (2013).
20. Fu, G. K. & Markovitz, D. M. The human LON protease binds to mitochondrial promoters in a single-stranded, site-specific, strand-specific manner. *Biochemistry* **37**(7), 1905–1909 (1998).
21. Yang, Q. et al. LONP-1 and ATFS-1 sustain deleterious heteroplasmy by promoting mtDNA replication in dysfunctional mitochondria. *Nat Cell Biol* **24**(2), 181–193 (2022).
22. Lu, B. et al. Phosphorylation of human TFAM in mitochondria impairs DNA binding and promotes degradation by the AAA+ Lon protease. *Mol Cell* **49**(1), 121–132 (2013).
23. Liu, T. et al. DNA and RNA binding by the mitochondrial lon protease is regulated by nucleotide and protein substrate. *J Biol Chem* **279**(14), 13902–13910 (2004).
24. Gibellini, L. et al. Sirtuin 3 interacts with Lon protease and regulates its acetylation status. *Mitochondrion* **18**, 76–81 (2014).
25. Bota, D. A. & Davies, K. J. Mitochondrial Lon protease in human disease and aging: Including an etiologic classification of Lon-related diseases and disorders. *Free Radic Biol Med* **100**, 188–198 (2016).
26. He, Y. et al. LONP1 downregulation with ageing contributes to osteoarthritis via mitochondrial dysfunction. *Free Radic Biol Med.* **191**, 176–190 (2022).
27. Hoshino, A. et al. Oxidative post-translational modifications develop LONP1 dysfunction in pressure overload heart failure. *Circ Heart Fail* **7**(3), 500–509 (2014).
28. Zanini, G. et al. The Role of Lonp1 on Mitochondrial Functions during Cardiovascular and Muscular Diseases. *Antioxidants (Basel)* **12**(3), 598 (2023).
29. Zhang, C. et al. LONP1 alleviates ageing-related renal fibrosis by maintaining mitochondrial homeostasis. *J Cell Mol Med* **28**(17), e70090 (2024).
30. Xu, Z. et al. Disuse-associated loss of the protease LONP1 in muscle impairs mitochondrial function and causes reduced skeletal muscle mass and strength. *Nat Commun* **13**(1), 894 (2022).
31. Gibellini, L. et al. Evidence for mitochondrial Lonp1 expression in the nucleus. *Sci Rep* **12**(1), 10877 (2022).
32. Pinti, M. et al. Emerging role of Lon protease as a master regulator of mitochondrial functions. *Biochim Biophys Acta* **1857**(8), 1300–1306 (2016).
33. Bahat, A. et al. Transcriptional activation of LON Gene by a new form of mitochondrial stress: A role for the nuclear respiratory factor 2 in StAR overload response (SOR). *Mol Cell Endocrinol* **408**, 62–72 (2015).
34. Pinti, M. et al. Functional characterization of the promoter of the human Lon protease gene. *Mitochondrion* **11**(1), 200–206 (2011).
35. Kalvala, A. K., Yerra, V. G. & Kumar, A. LONP1 induction by SRT1720 attenuates mitochondrial dysfunction against high glucose induced neurotoxicity in PC12 cells. *Toxicol In Vitro* **62**, 104695 (2020).
36. Torres, R. F., Kouro, R. & Kerr, B. Writers and Readers of DNA Methylation/Hydroxymethylation in Physiological Aging and Its Impact on Cognitive Function. *Neural Plast* **2019**, 5982625 (2019).
37. Gruzjeva, O. et al. Epigenome-Wide Meta-Analysis of Methylation in Children Related to Prenatal NO<sub>2</sub> Air Pollution Exposure. *Environ Health Perspect* **125**(1), 104–110 (2017).
38. Helliwell, A. M. et al. Changes in DNA methylation profiles of myalgic encephalomyelitis/chronic fatigue syndrome patients reflect systemic dysfunctions. *Clin Epigenetics* **12**(1), 167 (2020).
39. Tillotson, R. & Bird, A. The Molecular Basis of MeCP2 Function in the Brain. *J Mol Biol* **432**(6), 1602–1623 (2020).
40. Pecorelli, A. et al. Genes related to mitochondrial functions, protein degradation, and chromatin folding are differentially expressed in lymphomonocytes of Rett syndrome patients. *Mediators Inflamm* **2013**, 137629 (2013).
41. Cheng, T. L. et al. Regulation of mRNA splicing by MeCP2 via epigenetic modifications in the brain. *Sci Rep* **7**, 42790 (2017).
42. Pal, S. et al. A next-generation dynamic programming language Julia: Its features and applications in biological science. *J Adv Res* **64**, 143–154 (2024).
43. Sestakova, S., Salek, C. & Remesova, H. DNA Methylation Validation Methods: a Coherent Review with Practical Comparison. *Biol Proced Online* **21**, 19 (2019).
44. Li, L. C. & Dahiya, R. MethPrimer: designing primers for methylation PCRs. *Bioinformatics* **18**(11), 1427–1431 (2002).
45. Larsen, F. et al. CpG islands as gene markers in the human genome. *Genomics* **13**(4), 1095–1107 (1992).
46. Ponger, L. & Mouchiroud, D. CpGProD: identifying CpG islands associated with transcription start sites in large genomic mammalian sequences. *Bioinformatics* **18**(4), 631–633 (2002).
47. Torres, R. F. & Kerr, B. Spatial Learning Is Associated with Antagonist Outcomes for DNA Methylation and DNA Hydroxymethylation in the Transcriptional Regulation of the Ryanodine Receptor 3. *Neural Plast* **2021**, 9930962 (2021).
48. Okano, M. et al. DNA methyltransferases Dnmt3a and Dnmt3b are essential for de novo methylation and mammalian development. *Cell* **99**(3), 247–257 (1999).
49. Weirauch, M. T. et al. Determination and inference of eukaryotic transcription factor sequence specificity. *Cell* **158**(6), 1431–1443 (2014).
50. Grant, C. E., Bailey, T. L. & Noble, W. S. FIMO: scanning for occurrences of a given motif. *Bioinformatics* **27**(7), 1017–1018 (2011).
51. Bailey, T. L. et al. The MEME Suite. *Nucleic Acids Res* **43**(W1), W39–49 (2015).
52. Torres, R. F., Hidalgo, C. & Kerr, B. Mecp2 Mediates Experience-Dependent Transcriptional Upregulation of Ryanodine Receptor Type-3. *Front Mol Neurosci* **10**, 188 (2017).
53. Montecinos-Oliva, C. et al. Hormetic-Like Effects of L-Homocysteine on Synaptic Structure, Function, and Abeta Aggregation. *Pharmaceuticals (Basel)* **13**(2), 24 (2020).
54. Telese, F. et al. LRP8-Reelin-Regulated Neuronal Enhancer Signature Underlying Learning and Memory Formation. *Neuron* **86**(3), 696–710 (2015).
55. Lee, Y. G. et al. LONP1 and ClpP cooperatively regulate mitochondrial proteostasis for cancer cell survival. *Oncogenesis* **10**(2), 18 (2021).
56. Qi, X. et al. Epigenome-wide association study of Chinese monozygotic twins identifies DNA methylation loci associated with estimated glomerular filtration rate. *J Transl Med* **23**(1), 101 (2025).
57. Aerts, S. et al. Comprehensive analysis of the base composition around the transcription start site in Metazoa. *BMC Genomics* **5**(1), 34 (2004).
58. Xiao, F. H., Wang, H. T. & Kong, Q. P. Dynamic DNA Methylation During Aging: A “Prophet” of Age-Related Outcomes. *Front Genet* **10**, 107 (2019).
59. Weirauch, M. T. et al. Evaluation of methods for modeling transcription factor sequence specificity. *Nat Biotechnol* **31**(2), 126–134 (2013).
60. Kulakovskiy, I. V. et al. HOCOMOCO: a comprehensive collection of human transcription factor binding sites models. *Nucleic Acids Res* **41**(Database issue), D195–202 (2013).

61. Bach, S. et al. Methyl-CpG-binding protein 2 mediates overlapping mechanisms across brain disorders. *Sci Rep* **10**(1), 22255 (2020).
62. Drewell, R. A. et al. Methylation-dependent silencing at the H19 imprinting control region by MeCP2. *Nucleic Acids Res* **30**(5), 1139–1144 (2002).
63. Tai, D. J. et al. MeCP2 SUMOylation rescues Mecp2-mutant-induced behavioural deficits in a mouse model of Rett syndrome. *Nat Commun* **7**, 10552 (2016).
64. Tao, J. et al. Phosphorylation of MeCP2 at Serine 80 regulates its chromatin association and neurological function. *Proc Natl Acad Sci U S A* **106**(12), 4882–4887 (2009).
65. Zhou, Z. et al. Brain-specific phosphorylation of MeCP2 regulates activity-dependent Bdnf transcription, dendritic growth, and spine maturation. *Neuron* **52**(2), 255–269 (2006).
66. Zanini, G. et al. Differential Expression of Lonp1 Isoforms in Cancer Cells. *Cells* **11**(23), 3940 (2022).
67. Wu, L. et al. Sirt3 restricts tumor initiation via promoting LONP1 deacetylation and K63 ubiquitination. *J Transl Med* **21**(1), 81 (2023).
68. Ghosh, J. C. et al. Akt phosphorylation of mitochondrial Lonp1 protease enables oxidative metabolism and advanced tumor traits. *Oncogene* **38**(43), 6926–6939 (2019).
69. Kisselev, A. F. & Goldberg, A. L. Proteasome inhibitors: from research tools to drug candidates. *Chem Biol* **8**(8), 739–758 (2001).
70. Ryzhikov, S. & Bahr, B. A. Gephyrin alterations due to protein accumulation stress are reduced by the lysosomal modulator Z-Phe-Ala-diazomethylketone. *J Mol Neurosci* **34**(2), 131–139 (2008).
71. Hernando-Herraez, I. et al. Ageing affects DNA methylation drift and transcriptional cell-to-cell variability in mouse muscle stem cells. *Nat Commun* **10**(1), 4361 (2019).
72. Sahay, D., Terry, M. B. & Miller, R. Is breast cancer a result of epigenetic responses to traffic-related air pollution? A review of the latest evidence. *Epigenomics* **11**(6), 701–714 (2019).
73. Bird, A. DNA methylation patterns and epigenetic memory. *Genes Dev* **16**(1), 6–21 (2002).
74. Feng, J. et al. Role of Tet1 and 5-hydroxymethylcytosine in cocaine action. *Nat Neurosci* **18**(4), 536–544 (2015).
75. Hammerling, B. C. & Gustafsson, A. B. Mitochondrial quality control in the myocardium: cooperation between protein degradation and mitophagy. *J Mol Cell Cardiol* **75**, 122–130 (2014).
76. Pinti, M. et al. Mitochondrial Lon protease at the crossroads of oxidative stress, ageing and cancer. *Cell Mol Life Sci* **72**(24), 4807–4824 (2015).
77. Polo, M. et al. Lon protease: a novel mitochondrial matrix protein in the interconnection between drug-induced mitochondrial dysfunction and endoplasmic reticulum stress. *Br J Pharmacol* **174**(23), 4409–4429 (2017).
78. Wang, Q. et al. Perfluorooctanoic acid induces hepatocellular endoplasmic reticulum stress and mitochondrial-mediated apoptosis in vitro via endoplasmic reticulum-mitochondria communication. *Chem Biol Interact* **354**, 109844 (2022).
79. Anisimova, A. S. et al. Protein synthesis and quality control in aging. *Aging (Albany NY)* **10**(12), 4269–4288 (2018).
80. Liang, V. et al. Altered proteostasis in aging and heat shock response in *C. elegans* revealed by analysis of the global and de novo synthesized proteome. *Cell Mol Life Sci* **71**(17), 3339–3361 (2014).
81. Liu, W. et al. MicroRNA-16 targets amyloid precursor protein to potentially modulate Alzheimer's-associated pathogenesis in SAMP8 mice. *Neurobiol Aging* **33**(3), 522–534 (2012).
82. Granot, Z. et al. Turnover of mitochondrial steroidogenic acute regulatory (StAR) protein by Lon protease: the unexpected effect of proteasome inhibitors. *Mol Endocrinol* **21**(9), 2164–2177 (2007).
83. Quiros, P. M. et al. ATP-dependent Lon protease controls tumor bioenergetics by reprogramming mitochondrial activity. *Cell Rep* **8**(2), 542–556 (2014).
84. Lee, J. et al. Inhibition of mitochondrial LonP1 protease by allosteric blockade of ATP binding and hydrolysis via CDDO and its derivatives. *J Biol Chem* **298**(3), 101719 (2022).
85. Ehlers, M. D. Activity level controls postsynaptic composition and signaling via the ubiquitin-proteasome system. *Nat Neurosci* **6**(3), 231–242 (2003).
86. Diering, G. H. & Huganir, R. L. The AMPA Receptor Code of Synaptic Plasticity. *Neuron* **100**(2), 314–329 (2018).
87. Meiners, S. et al. Inhibition of proteasome activity induces concerted expression of proteasome genes and de novo formation of Mammalian proteasomes. *J Biol Chem* **278**(24), 21517–21525 (2003).
88. Vousden, K. H. & Lane, D. P. p53 in health and disease. *Nat Rev Mol Cell Biol* **8**(4), 275–283 (2007).
89. Musgrove, E. A. et al. Cyclin D as a therapeutic target in cancer. *Nat Rev Cancer* **11**(8), 558–572 (2011).

## Author contributions

J.L. and C.T.-R. wrote the main manuscript text and J.L., K.C., C.J., C.V., and A.S. prepared Figs. 1–3. All authors reviewed the manuscript.

## Funding

This work was supported by ANID 21212277 to JL, ANID FONDECYT 1230905 to BK, ANID FONDECYT 11241376 to CJ, ANID FONDECYT 1241935 to MKSH, FONDECYT 1221178 to CTR and Centro Ciencia & Vida, FB210008, Financiamiento Basal para Centros Científicos y Tecnológicos de Excelencia ANID to CTR and AL.

## Declarations

## Competing interests

The authors declare no competing interests.

## Institutional Review Board

The experimental procedures were approved by the Bioethical and Biosafety Committee of the University of San Sebastian, Chile, under CEC N° 23–2021–20 and 0001–04–04–22.

## Additional information

**Supplementary Information** The online version contains supplementary material available at <https://doi.org/10.1038/s41598-025-24766-2>.

**Correspondence** and requests for materials should be addressed to B.K. or C.T.-R.

**Reprints and permissions information** is available at [www.nature.com/reprints](http://www.nature.com/reprints).

**Publisher's note** Springer Nature remains neutral with regard to jurisdictional claims in published maps and institutional affiliations.

**Open Access** This article is licensed under a Creative Commons Attribution-NonCommercial-NoDerivatives 4.0 International License, which permits any non-commercial use, sharing, distribution and reproduction in any medium or format, as long as you give appropriate credit to the original author(s) and the source, provide a link to the Creative Commons licence, and indicate if you modified the licensed material. You do not have permission under this licence to share adapted material derived from this article or parts of it. The images or other third party material in this article are included in the article's Creative Commons licence, unless indicated otherwise in a credit line to the material. If material is not included in the article's Creative Commons licence and your intended use is not permitted by statutory regulation or exceeds the permitted use, you will need to obtain permission directly from the copyright holder. To view a copy of this licence, visit <http://creativecommons.org/licenses/by-nc-nd/4.0/>.

© The Author(s) 2025